

RSC Advances



This is an *Accepted Manuscript*, which has been through the Royal Society of Chemistry peer review process and has been accepted for publication.

Accepted Manuscripts are published online shortly after acceptance, before technical editing, formatting and proof reading. Using this free service, authors can make their results available to the community, in citable form, before we publish the edited article. This *Accepted Manuscript* will be replaced by the edited, formatted and paginated article as soon as this is available.

You can find more information about *Accepted Manuscripts* in the [Information for Authors](#).

Please note that technical editing may introduce minor changes to the text and/or graphics, which may alter content. The journal's standard [Terms & Conditions](#) and the [Ethical guidelines](#) still apply. In no event shall the Royal Society of Chemistry be held responsible for any errors or omissions in this *Accepted Manuscript* or any consequences arising from the use of any information it contains.

Cite this: DOI: 10.1039/coxx00000x

www.rsc.org/xxxxxx

ARTICLE TYPE

Synthesis and Discovery of Andrographolide Derivatives as Non-steroidal Farnesoid X Receptor (FXR) Antagonists

Zhuyun Liu,^{a,§} Wai-Kit Law,^b Decai Wang,^a Xin Nie,^a Dekuan Sheng,^a Genrui Song,^a Kai Guo,^c Ping Wei,^c Pingkai Ouyang,^c Chi-Wai Wong,^{*,b} Guo-Chun Zhou^{*,a}

[§] Received (in XXX, XXX) Xth XXXXXXXXX 20XX, Accepted Xth XXXXXXXXX 20XX

DOI: 10.1039/b000000x

Based upon the discovery of natural compound andrographolide (**1**) as a non-steroidal farnesoid X Receptor (FXR) antagonist, a series of andrographolide derivatives were designed and synthesized accordingly. Our primary SAR studies demonstrated that 14-phenoxy andrographolide scaffold is an excellent structural pharmacophore for FXR antagonists. Remarkably, 14 β -compounds of **12b**, **12f** and **10g** were found to be the most potent FXR antagonists in this work. Structural docking discovered that the phenoxy substitution at 14-position and the modification at 3,19-positions altered the putative binding poses of small FXR ligands, resulting in their FXR antagonistic activity discrepancy.

Introduction

Nuclear receptors are classified as ligand-activated transcription factors that regulate the expression of specific target genes and are involved in several physiological functions including reproduction, development, and metabolism.¹ Farnesoid X receptor (FXR), also known as bile acid receptor (BAR) or NR1H4, is a nuclear receptor that is encoded by the *NR1H4* gene in human and expressed at high levels in the liver, intestine and other cholesterol-rich tissues.^{1,2} Cholic acid (CA), chenodeoxycholic acid (CDCA), and other bile acids are natural ligands²⁻⁵ for FXR (Figure 1).

After activated by bile acid ligand/s,²⁻⁵ FXR translocates to the cell nucleus, where FXR recruits retinoid X receptor (RXR) to form a heterodimer and then binds to hormone response elements on DNA, which up- or down-regulates the expression of certain genes.^{1,2} The downregulation of CYP7A1²¹ (cholesterol 7 α -hydroxylase) of the rate-limiting enzyme in bile acid synthesis from cholesterol is one of the primary functions of FXR activation, resulting in a negative feedback in which synthesis of bile acids is inhibited if the cellular levels of bile acids are high.¹⁻⁵ It is reported that FXR has an active role in regulating cholesterol, lipoprotein, and glucose metabolism and its association with liver disease,^{22,23} liver regeneration²⁴ and tumorigenesis,²⁵ suggesting that FXR represents an attractive pharmacological target.^{26,27}

Currently, most studies are focused on FXR agonists (Figure 1). Because it is possible that FXR over-regulation causes some diseases and an unnatural FXR agonist diverts the normal pathway to result in potentially undesirable side effects,²⁵⁻²⁸ it is necessary to develop FXR antagonists as FXR modulators.

The known FXR antagonists (Figure 1) are mainly derived from steroidal scaffold and a finite of other structural skeletons

are reported in recent years. Thus, seeking potent, structurally diverse and non-steroidal FXR antagonists should be an important direction in the field. The utilization of natural products as a source of structural or functional diversity for the design and synthesis of novel molecules has been an important aspect of new drug design.^{29,30} So as to increase structural diversity of FXR antagonists, we launched a project initiated by the high-throughput screening of the natural compound libraries from a series of the Traditional Chinese Medicines (TCMs) based on FXR luciferase activity assay.³¹ Andrographolide (**1**, Figure 1),^{32,33} a diterpene ester from *Andrographis paniculata* (Burm.f.) Nees, was identified as a weak FXR antagonist (IC₅₀ = 9.7 μ M, Figure 2).

Andrographolide (**1**) is the representative active ingredient of *Andrographis paniculata* (Burm.f.) Nees and it works as a broad therapeutic agent.^{34,35} Although **1** has 350 dalton of molecular weight, 3 hydrogen bond donors, 5 hydrogen bond acceptors and 2.1186 of the calculated LogP (Table s1, entry 23), which conforms the "Rule of Five", its poor water-solubility and also relatively low lipo-solubility, weak potency and inadequate therapeutic efficacy restrict its further application. To improve its physiochemical properties and pharmaceutical features, numerous andrographolide derivatives were reported from time to time, especially preparation of 14-acyloxy andrographolide derivatives³⁶⁻⁴⁰ (**2**, Figure 1). Herein, we describe the synthesis and SAR studies of 14-aryloxy andrographolide derivatives (**3** and **4**, Figure 1), leading to the identification of a series of 14-phenoxy andrographolide derivatives as more potent FXR antagonists than the lead andrographolide (**1**).⁴¹

Results and discussion

In our preliminary study, andrographolide (**1**) was found to be a weak FXR antagonist (IC₅₀ = 9.7 μ M) in the concentration-

dependent mode (Figure 2),³¹ this result spurred us to discover more potent FXR antagonists on the basis of andrographolide derivatives. As 14-acyloxy andrographolide esters (**2**, Figure 1)

were effective in some reported studies for other assays,³⁶⁻³⁸ we were interested in exploring 14-modified andrographolide derivatives as FXR novel antagonists.

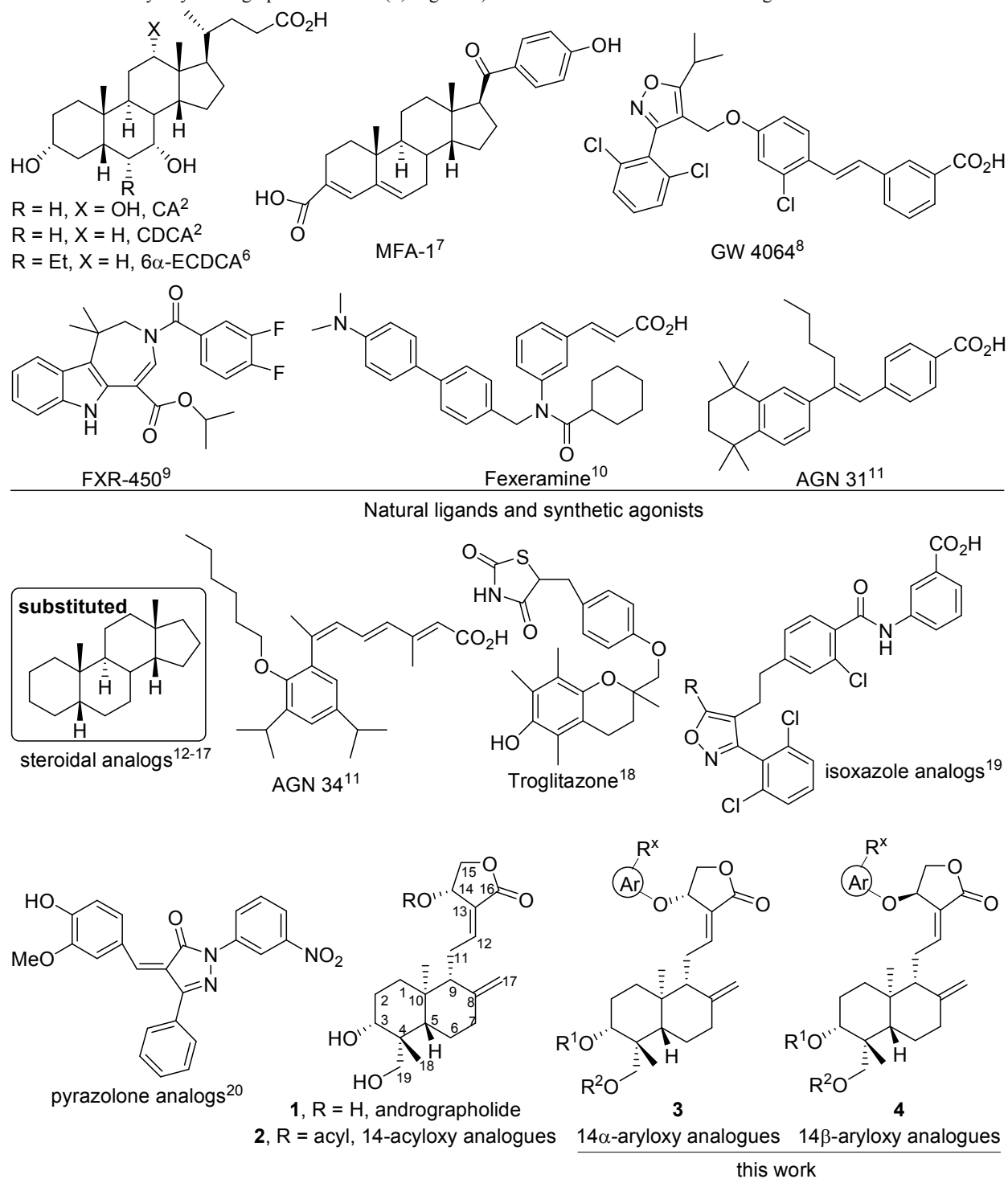
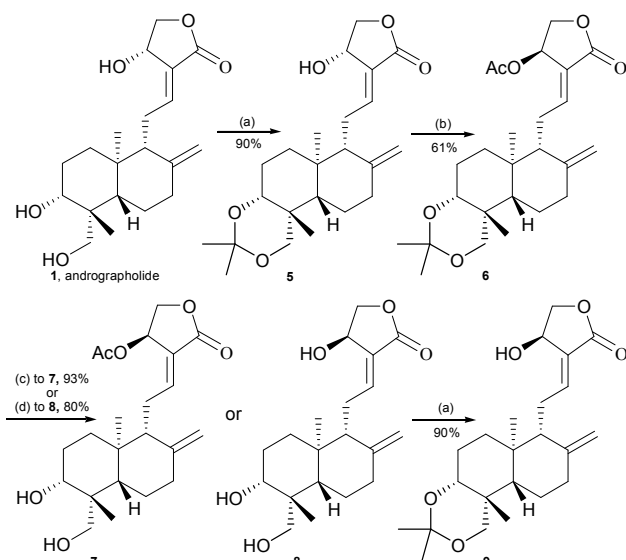


Figure 1. Natural and synthetic known ligands for FXR and general structures of andrographolide and their derivatives.

In initial exploration step, some simple derivatives of andrographolide were studied (Scheme 1). Starting from **1**, 3,19-acetonylidene protection was conducted in DCM and catalyzed by PPTS gave **5** as reported.³⁶⁻³⁸ Inversion of 14 α -OH of **5** into 14 β -OAc of **6** was achieved by Mitsunobu reaction under the

normal condition. 14-Epimeric andrographolide (**8**) or its 14 β -acetylated derivative (**7**) was generated in MeOH/H₂O (4/1) with TsOH·H₂O by partial (at 20 °C) or complete (40 °C) hydrolysis of **6**, respectively. Finally, 14 β -3,19-acetonylidene derivative (**9**) was made by the same preparation condition as **5**.

Scheme 1.^a

^aReagents and conditions: (a) anhydrous DCM, 2,2-dimethoxypropane, PPTS, 40 °C; (b) anhydrous THF; **5** (1.0 eq), anhydrous HOAc (1.5 eq), DIAD (1.5 eq), PPh₃ (1.5 eq), 0 °C to room temperature; (c) MeOH/H₂O (4/1), TsOH·H₂O, 20 °C; (d) MeOH/H₂O (4/1), TsOH·H₂O, 40 °C.

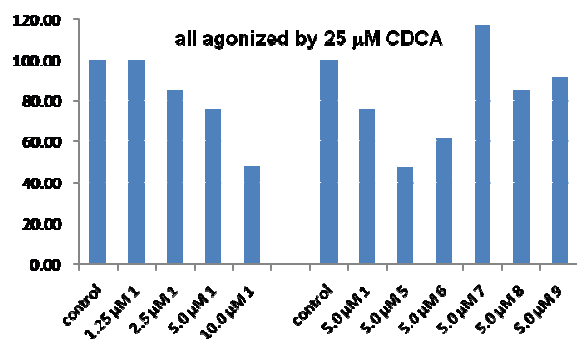
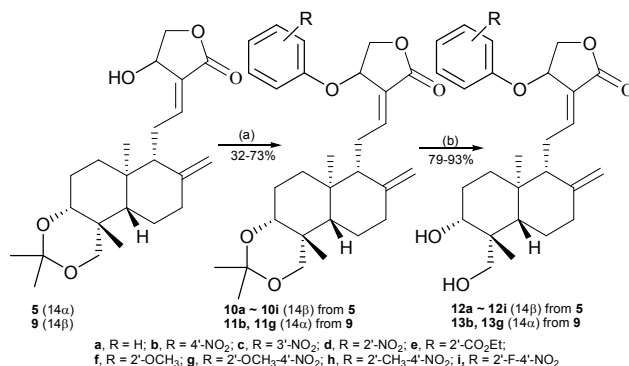


Figure 2. The FXR antagonistic activities of compounds **1** and **5-9**. Control (100%) is the activity of FXR in the presence of 25.0 μM CDCA.

FXR antagonistic results of the synthesized compounds were measured by the luciferase reporter assay³¹ and shown in Table 1 (entries 23-28). The antagonistic potencies at 5.0 μM were depicted in Figure 2. Compared to **1**, 3,19-isopropylidene andrographolide (**5**) slightly improved the FXR antagonistic activity. 14β-Epimeric andrographolide (**8**) was a much weaker FXR antagonist than **1** and 14β-acetylated andrographolide (**7**) became inactive to FXR. Unlike the relationship between **1** and **5**, 3,19-isopropylidene 14β-andrographolide (**9**) was indeed a weaker FXR antagonist than **8**. 14β-Acetylated 3,19-isopropylidene andrographolide (**6**) is more active than 14β-acetylated 3,9-diol analogue **7** in antagonizing FXR. By comparison of 14β-andrographolide (**8**) with its modified derivatives (**6**, **7**, **9**), it was discovered that 3,19-isopropylidene modification alone (**9**) almost did not change the antagonistic activity and 14-acetylation modification alone (**7**) decreased the antagonistic activity, but simultaneous modifications (**6**) of 3,19-isopropylidene and 14-acetylation enhanced somewhat the antagonistic activity. It was inferred from these preliminary data (Figure 2 and Table 1, entries 23-28) that the optimal combination of 3,19- and 14-modifications including 14α- or

14β-configuration is possibly helpful for the FXR antagonistic activity.

Considering that aryloxy ether is chemically more stable than acyloxy ester, we are interested in 14-aryloxy ether analogues of andrographolide (Figure 1) in our exploration. Increment of the structural diversity is the important superiority of 14-aryloxy ether by the utilizing of varied aromatic skeletons (e.g. phenyl, naphthyl, quinolinyl, pyridinyl, etc) and the incorporation of different substituents into aromatic scaffolds. In this work, 14-phenoxy andrographolide derivatives (Ar = Ph, Figure 1, series **3** and **4**) were firstly studied.

Scheme 2.^a

^aReagents and conditions: (a) anhydrous THF; **5** or **9** (1.0 eq), phenol (1.5 eq), DIAD (1.5 eq), PPh₃ (1.5 eq), 0 °C to room temperature; (b) MeOH/H₂O (4/1), TsOH·H₂O, 20 °C.

As shown in Scheme 2, 14α-compound **5** or its 14β-epimer **9** were used as starting materials for the synthesis of 14β- or 14α-phenoxy andrographolide derivatives, respectively. The key synthetic approach to 14-phenoxy andrographolide derivatives is Mitsunobu reaction. Diverse phenols were used to prepare two series of 14β-phenoxy (**10**) and 14α-phenoxy (**11**) compounds. The reaction was performed as general from 0 °C to room temperature in anhydrous THF and afforded **10** or **11** in mild to moderate isolated yield depending on distinct phenol property. Removal of the protective group of 3,19-acetylidene from **10** or **11** by TsOH·H₂O in MeOH/H₂O (4/1) at 20 °C, the series of compounds **12** or **13** were obtained in high yields, respectively. It is worthwhile to note that α-isomers of **11** and **13** were generally less stable than their corresponding β-isomers of **10** and **12**.

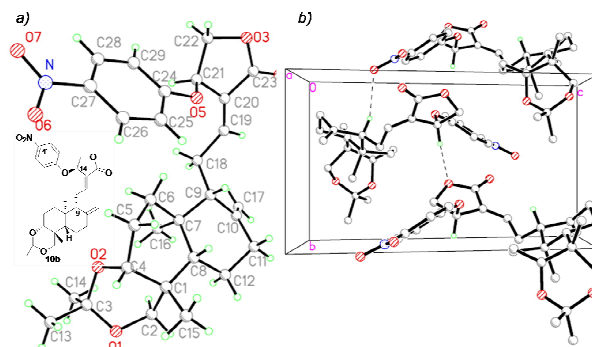


Figure 3. Molecular and crystal structures (a) and crystal packing diagram (b) of **10b**. The crystal structure was deposited at the Cambridge Crystallographic Data Centre and deposition numbers is CCDC 960845.

In order to confirm the stereochemistry of C-14 in these series, the single crystal of **10b** was cropped from petroleum

ether/ethyl acetate (5/4) and its crystal structure was determined as shown in Figure 3a by the X-ray crystallography, which is in accordance with our expected structure. The crystal packing diagram (Figure 3b) of **10b** demonstrated that the molecule **10b** is stabilized and chained by the intermolecular hydrogen bonds of C(9)-H(β) \cdots O(4'-NO₂) and C(14)-H(α) \cdots O(lactone)-C(15).

The calculated data of "Lipinski's Rule of Five" of **1** and these synthesized compounds **5-9** and **10-13** are included in Table S1. Even some of these compounds do not conform very well the "Rule of Five", they have potentials to be optimized and developed into drug-like candidates in the future. FXR antagonistic activity and the cellular toxicity of **1** and these synthesized compounds **5-9**, and **10-13** are listed in Table 1.

Table 1. FXR antagonistic activity of synthesized compounds **1**, **5-9**, **10-13**

entry	compd ^{a)}	R	14-isomer	IC ₅₀ ^{b)}	CC ₅₀ ^{c)}
1	10a	H	β	NA	-
2	12a	H	β	5.7	> 15.0
3	10b	4'-NO ₂	β	8.6	> 15.0
4	12b	4'-NO ₂	β	0.55	> 15.0
5	10c	3'-NO ₂	β	NA	-
6	12c	3'-NO ₂	β	NA	-
7	10d	2'-NO ₂	β	3.0	8.5
8	12d	2'-NO ₂	β	NA	-
9	10e	2'-CO ₂ Et	β	2.9	12.3
10	12e	2'-CO ₂ Et	β	3.5	> 15.0
11	10f	2'-OCH ₃	β	2.4	> 15.0
12	12f	2'-OCH ₃	β	0.98	> 15.0
13	10g	2'-OCH ₃ -4'-NO ₂	β	2.0	> 15.0
14	12g	2'-OCH ₃ -4'-NO ₂	β	11.9	> 15.0
15	10h	2'-CH ₃ -4'-NO ₂	β	6.3	> 15.0
16	12h	2'-CH ₃ -4'-NO ₂	β	NA	-
17	10i	2'-F-4'-NO ₂	β	3.9	> 15.0
18	12i	2'-F-4'-NO ₂	β	NA	-
19	11b	4'-NO ₂	α	15.1	> 15.0
20	13b	4'-NO ₂	α	16.0	> 15.0
21	11g	2'-OCH ₃ -4'-NO ₂	α	2.5	12.0
22	13g	2'-OCH ₃ -4'-NO ₂	α	7.1	> 15.0
23	1, andrographolide		α	9.7	> 15.0-
24	5		α	9.0	> 15.0
25	6		β	9.3	> 15.0
26	7		β	NA	-
27	8		β	> 15.0	-
28	9		β	> 15.0	-

^{a)} See Scheme 2. ^{b)} FXR-transfected 293T cells were agonized by 25.0 μ M CDCA in all experiments and the vehicle control was set as 100%, "NA" means "not active". ^{c)} The 293T cells were used to test compound's cellular toxicity, "-" represents "not detected".

At first, 14 β -phenoxy andrographolide derivative **10a** bearing 3,19-acetylidenylidene group was found to be inactive (Table 1, entry 1); however, its hydrolyzed product of 3,19-diol **12a** (Table 1, entry 2) exhibited as a moderate FXR antagonist (IC₅₀ = 5.7 μ M), which is better than our lead **1**. Then, we moved to incorporate substituted groups into phenyl ring at 14-position to investigate the structure-activity relationship (SAR). 4'-Nitrophenoxy compounds of **10b** with 3,19-acetylidenylidene group

and **12b** of 3,19-diol derivative were designed and tested. Compound **10b** (IC₅₀ = 8.6 μ M; Table 1, entry 3) is less potent than **12a** but it is much more active than its corresponding counterpart **10a** as a FXR antagonist; notably, IC₅₀ value of **12b** reached 0.55 μ M (Table 1, entry 4) in the FXR antagonistic activity, indicating that 14-(4'-nitrophenoxy) group is an important pharmacophore (**10a** < **10b** and **12a** < **12b**). In addition, it seems that 3,19-acetylidenylidene group decreases the FXR antagonistic activity (**10a** < **12a** and **10b** < **12b**) for these compounds.

After the above, 3'- and 2'-nitrophenoxy andrographolide derivatives **10c** and **12c**, **10d** and **12d**, respectively, were designed to investigate the effects of different nitro positions on the FXR antagonistic activity in comparison to 4'-nitrophenoxy analogues **10b** and **12b**. Among these, **10c** and **12c** of 3'-nitrophenoxy analogues, and **12d** of 2'-nitrophenoxy analogue did not express the FXR antagonistic activity (Table 1, entries 5, 6 and 8); nevertheless, **10d** of 2'-nitrophenoxy analogue with 3,19-acetylidenylidene (Table 1, entry 7) showed a good FXR antagonistic activity (IC₅₀ = 3.0 μ M) but it possessed an obvious cellular toxicity (CC₅₀ = 8.5 μ M). Based upon these results, we further explored other substitution at 2'-position of 14-phenoxy group. Compound **10e** with an electron-withdrawing group of 2'-carboxylic ester (Table 1, entry 9) exhibited the close FXR antagonistic activity (IC₅₀ = 2.9 μ M) and similar cellular toxicity (CC₅₀ = 12.3 μ M) to its 2'-nitro counterpart **10d**. 2'-Carboxylic ester 3,19-diol compound **12e** (Table 1, entry 10), which is different from its inactive 2'-nitro-3,19-diol counterpart **12d**, acted as a good FXR antagonist (IC₅₀ = 3.5 μ M) but did not show obvious cellular toxicity. Interestingly, an electron-donating group of 2'-methoxy-substituted compound **10f** with 3,19-acetylidenylidene exhibited the similar FXR antagonistic activity (IC₅₀ = 2.4 μ M, Table 1, entry 11) to **10d** and **10e** containing 2'-electron-withdrawing substitutions. Moreover, 2'-methoxy-3,19-diol **12f** was very active (IC₅₀ = 0.98 μ M, Table 1, entry 12) and its relatively low cellular toxicity was detected. Summarized from the above-mentioned results, it is concluded that the mono substitution at 2'-position is very flexible to the electron-donating group and the electron-withdrawing group for the FXR antagonistic activity, especially for **10** series compounds with 3,19-acetylidenylidene group.

Inspired by these promising results of **12b** and **12f** bearing 4'-nitro group and 2'-methoxy group at 14-phenoxy, respectively, 2'-methoxy-4'-nitro-andrographolide derivatives **10g** and **12g** were logically designed (Figure 4) and tested for their FXR antagonistic activity (Table 1 and Figure 4). We envisioned that the "integration" of 2'-methoxy and 4'-nitro groups should retain or increase the antagonistic activity. Compared to its mother analogues **10b** (4'-nitro) and **10f** (2'-methoxy) with single substitution at 14-phenoxy, dual substituted 2'-OMe-4'-NO₂ derivative **10g** with 3,19-acetylidenylidene (IC₅₀ = 2.0 μ M, Figure 4 and Table 1, entry 13) was more potent FXR antagonist than **10b** (IC₅₀ = 8.6 μ M) and **10f** (IC₅₀ = 2.4 μ M) as expected. However, it is surprised that 3,19-diol **12g** (IC₅₀ = 11.9 μ M) with dual substitutions at 14-phenoxy by 2'-methoxy group and 4'-nitro group (Figure 4 and Table 1, entry 14) showed much weaker FXR antagonistic activity than **10g** and its corresponding mother

3,19-diol analogues **12b** and **12f**, suggesting that the “integration” of 2'-methoxy and 4'-nitro groups affects the binding ability of these small molecules to FXR. More importantly, these data reveal that there are synergistic effects between substitutions at 14-phenoxy and 3,19-modifications on the antagonistic activities to the receptor FXR.

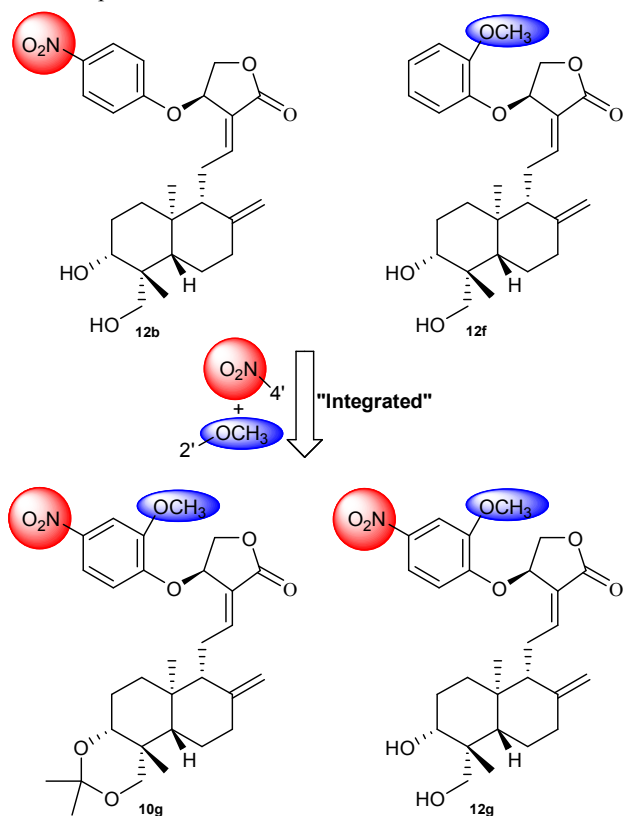


Figure 4. Design of **10g** and **12g** from **12b** and **12f**.

As a part of exploring the effects of 14-phenoxy substitutions on the FXR antagonistic activity, substituents of methyl group as a weak electron-donating group and fluoro group as an electron-withdrawing group were introduced at 2'-position into 14-(4'-nitro)-phenoxy group, respectively. The assay data disclosed that 2'-methyl-4'-nitro derivative **10h** was a moderate FXR antagonist ($IC_{50} = 6.3 \mu\text{M}$, Table 1, entry 15) and its diol derivative **12h** lost FXR antagonistic activity (Table 1, entry 16); meanwhile, introduction of 2'-fluoro at 14-(4'-nitro)-phenoxy made **10i** bearing 3,19-acetonilidene ($IC_{50} = 3.9 \mu\text{M}$, Table 1, entry 17) be slightly more active than 2'-methyl counterpart **10h** but its diol analogues **12i** (Table 1, entry 18) was lack of FXR antagonistic activity as 2'-methyl counterpart diol **12h**.

Taking into consideration that **1** is a 14 α -isomer, we subsequently investigated 14 α -(4'-nitro-phenoxy) and 14 α -(2'-methoxy-4'-nitro-phenoxy) andrographolide analogues (Scheme 2 and Table 1, entries 19-22) since their corresponding 14 β -isomers **12b** and **12g** are very potent FXR antagonists. Contrary to their 14 β -isomers of **10b** and **12b**, two 14 α -(4'-nitro)-phenoxy analogues of **11b** ($IC_{50} = 15.1 \mu\text{M}$, Table 1, entry 19) and **13b** ($IC_{50} = 16.0 \mu\text{M}$, Table 1, entry 20) were unfortunately weaker FXR antagonists than **1** ($IC_{50} = 9.7 \mu\text{M}$). **11g** ($IC_{50} = 2.5 \mu\text{M}$, Table 1, entry 21) of 3,19-acetonilidene-14 α -(2'-methoxy-4'-nitro)-phenoxy derivative showed close FXR antagonistic activity

to its 14 β -counterpart **10g** ($IC_{50} = 2.0 \mu\text{M}$) but **11g** exhibited a cellular toxicity ($CC_{50} = 12.0 \mu\text{M}$); meanwhile, its corresponding diol **13g** ($IC_{50} = 7.1 \mu\text{M}$, Table 1, entry 22) was a moderate FXR antagonist. Thus, these data together with their less stability suggest that at the current stage, 14 α -isomer analogues were not considered further to be FXR antagonists.

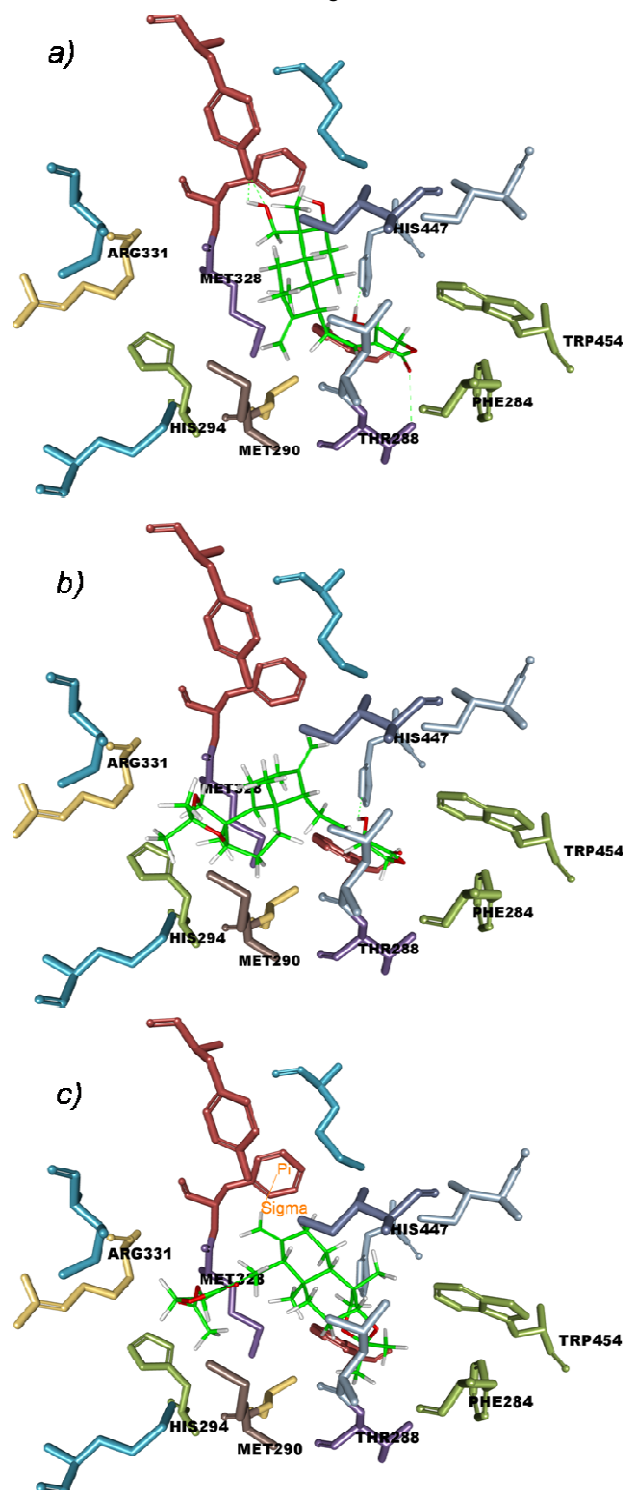


Figure 5. Three-dimensional (3D) interaction diagrams of predicted binding poses of **1** (a), **5** (b) and **6** (c) in FXR active sites. Critical amino acid residues of the binding pocket are labelled. The green dash line denotes hydrogen bond between ligand and amino acid residue atoms of FXR protein.

To decipher the structural basis for the above SARs, we compared the putative binding poses of compounds **1**, **5**, **6**, **10b**, **12b**, **10g** and **12g** by means of molecular docking. The docking

model was generated from the chain A of 3DCT⁴² from the same view using Discovery Studio 3.5 and the modelling results are shown in Figures 5 and 6.

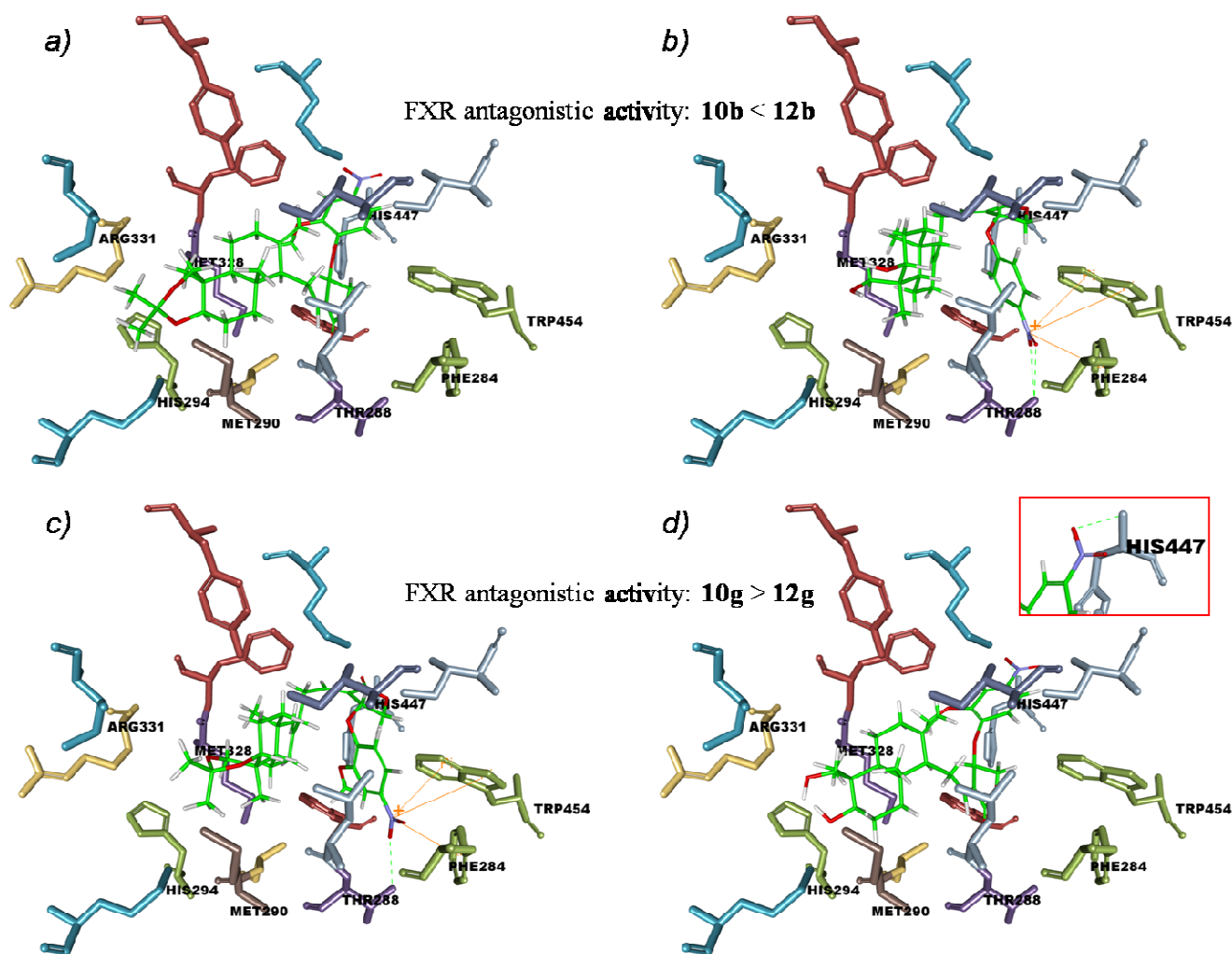


Figure 6. Three-dimensional (3D) interaction diagrams of predicted binding poses of **10b** (a), **12b** (b), **10g** (c) and **12g** (d) in FXR active site. Critical amino acid residues of the binding pocket are labelled. The green dash line denotes hydrogen bond between ligand and amino acid residue atoms of FXR protein, while the orange line denotes the π - π interaction from the ligand to amino acid aromatic ring residue of FXR protein. The inset (in red rectangle) of hydrogen bond in **12g** (d) was viewed from different visual angle.

As shown in Figure 5, even FXR antagonistic activities of **1**, **5** and **6** are close, the putative binding poses of **1** (Figure 5a), **5** (Figure 5b) and **6** (Figure 5c) in NS3 appear to be quite different, which their orientations of decalin rings are distinctive, the bindings of lactone rings in **1** and **5** are similar but different from that in **6**. The putative binding pose of **1** can be transformed into **5**'s by making a rotation of 180° along the bond of C9-C11 or C11-C12 or **6**'s by a rotation of 90° clockwise and then 180° along the bond of C9-C11 or C11-C12. These simulation results suggest that the spatial volume of the binding pocket in NS3 is large enough for different occupation modes which are dependent on the interaction between a specific ligand with the binding site. This means that optimal structural tuning will benefit binding potency.

Further, the predictive binding of the most potent compound of 3,19-diol **12b** is in a good accommodation to the large spatial volume binding pocket (Figure 6b), in which there are two

hydrogen bonds between 4'-nitro group and hydroxyl group of Thr 288 residue and three π - π interactions of 4'-nitro group with aromatic rings of Trp454 and Phe284, leading to the tight binding between **12b** and FXR (Figure 6b). However, due to the relative large and rigid 6-membered ring formed by 3,19-acetonilidene protection as indicated in Figure 6a, compound **10b**, whose binding pose is close to **5** but not **1** or **6**, was obstructed by the putative "gate" established by 4 amino acid residues of Met290, His294, Met328 and Arg331, which lets compound **10b** not fully enter the binding pocket, resulting in the loss of hydrogen bond and π - π interaction in the binding of **10b** to FXR. These molecular binding poses of **10b** and **12b** are in good agreement with their FXR antagonistic activities (**10b** < **12b**). Moreover, by comparison with the predictive binding poses of **10b** and **12b**, the orientations of 14 β -(4'-nitro)-phenoxy moiety and the lactone ring of **10b** are reciprocally exchanged, suggesting the importance of their orientations for the binding.

Since compounds **10g** and **12g** expressed big differences in their FXR antagonistic activities (**10g** > **12g**) and their SAR is totally distinct from that of **10b** and **12b** (**10b** < **12b**), we were interested in understanding how 2'-methoxy group affects the binding poses of **10g** and **12g**. Interestingly and notably, the predictive binding pose of **10g** (Figure 6c) bearing 3,19-acetylidene protective group is different from that of its corresponding counterpart **10b** (Figure 6a) but is quite similar to that of the diol **12b** (Figure 6b); meanwhile, the predictive binding pose of the diol **12g** (Figure 6d) is not similar to that of the diol **12b** (Figure 6b) but is almost identical to that of 3,19-acetylidene protected compound **10b** (Figure 6a), these observations gave a good explanation for the above-mentioned FXR antagonistic relationship of **10b** < **12b** vs **10g** > **12g** (Figure 6; Table 1, entries 1, 2, 13 and 14). Except for one more hydrogen bond in the binding pose of **12b** as shown in Figure 6b, the interaction of **10g** with FXR (Figure 6c), which is stabilized by one hydrogen bond and three π - π interactions, is similar to **12b**. Because 3,19-acetylidene protected molecule **10g** was partially blocked by the "gate" (Figure 6c), the binding pose of **10g** is much more flat than **12b** in order to reach the same binding site as **12b**. These results demonstrated that 2'-methoxy group plays an important role in the binding of these small molecules to FXR.

These modelling results are interesting that the putative binding poses of **10b** (14 β) and **12g** (14 β), and the putative orientations of decalin rings of **12b** (14 β) and **10g** (14 β) are close to those of **5** (14 α) but not **6** (14 β), respectively.

Conclusions

In summary, starting from easy-to-get natural compound of andrographolide (**1**), a series of andrographolide derivatives by the introduction of various substituted phenoxy groups to andrographolide at 14-position were straightforward synthesized with the inversion of 14-configuration by Mitsunobu reaction. Our primary SAR studies disclosed that 14-phenoxy andrographolide scaffold is an excellent structural moiety for FXR antagonists. Structural tuning of the substitutions at 14-phenoxy, modifications at 3,19-positions and 14-configurations could be an efficient way to discover 14-phenoxy andrographolide derivatives as effective FXR antagonists with low cellular toxicity. Remarkably, 14 β -compounds of **12b**, **12f** and **10g** were found to be the most potent FXR antagonists in this work. Less stability and relatively weaker potency with somewhat cellular toxicity of α -isomers restrict their application from our current data. The structural docking unveiled that the structural features of a small FXR ligand affects its binding pose, resulting in its FXR antagonistic discrepancy. It should be mentioned that these compounds have potentials to be optimized and developed into drug-like candidates in the future even compounds **6**, **10b-h**, **11b**, **11g** and **12h** have too high CLogP values (>5.0) to obey Lipinski rule of 5. Taken together, the data strongly support that andrographolide backbone combined with phenoxy substitution at 14-position provides an excellent scaffold for FXR antagonists.

Experimental

Materials and equipment

Unless otherwise noted, materials were obtained from commercial suppliers and used without further purification. Melting points were measured using an YRT-3 melting point apparatus (Shanghai, China) and were uncorrected. ^1H and ^{13}C NMR spectra were recorded on a Bruker AV-400 spectrometer at 400 and 100 MHz, respectively, in CDCl_3 , CD_3OD , $\text{DMSO}-d_6$, etc. as indicated. Coupling constants (J) are expressed in hertz (Hz). Chemical shifts (δ) of NMR are reported in parts per million (ppm) units relative to the solvent. The low or high resolution of ESIMS (in the positive ion or negative ion acquisition mode) was recorded on an Agilent 1200 HPLC-MSD mass spectrometer or Applied Biosystems Q-STAR Elite ESI-LC-MS/MS mass spectrometer, respectively.

Preparation of 3,19-acetylidene andrographolide (**5**)³⁶⁻³⁸

To the solution of 10g (28.5mmol) of andrographolide (**1**) and 24 ml (196mmol) of 2,2-dimethoxypropane in 20.0 ml of anhydrous dichloromethane, 0.72g (2.9 mmol) of PPTS was added and the reaction mixture was heated at 40 °C. The reaction was monitored by TLC and then treated with ethyl acetate and sat. NaHCO_3 after the reaction was complete. The organic phase was washed with brine, dried over anhydrous Na_2SO_4 , and then filtered organic solution was evaporated to dryness. The residue was purified by silica gel column chromatography (petroleum ether/ethyl acetate 1/1) to afford a white solid 10.05g (90.2%); m.p. 187-192 °C. ^1H NMR (400 MHz, $\text{DMSO}-d_6$) δ 6.63 (t, $J = 6.4$ Hz, 1H), 5.74 (d, $J = 6.0$ Hz, 1H), 4.93 (t, $J = 5.8$ Hz, 1H), 4.86 (s, 1H), 4.69 (s, 1H), 4.41 (dd, $J = 10.0, 6.0$ Hz, 1H), 4.04 (dd, $J = 9.8, 1.8$ Hz, 1H), 3.89 (d, $J = 11.6$ Hz, 1H), 3.42 (dd, $J = 9.2, 3.6$ Hz, 1H), 3.12 (d, $J = 11.6$ Hz, 1H), 2.54-2.50 (m, 1H), 2.40-1.88 (m, 3H), 1.78 - 1.63 (m, 3H), 1.34 (s, 3H), 1.26 (s, 3H), 1.34-1.15 (m, 3H), 1.14 (s, 3H), 0.88 (s, 3H).

Preparation of 3,19-acetylidene-14 β -acetoxy-andrographolide (**6**)

Under N_2 atmosphere, 1.0 mmol of compound **5**, 1.5 mmol of PPh_3 , 1.5 mmol of acetic acid were dissolved in 10.0 ml of anhydrous THF. The solution was cooled to 0 °C and then treated with 1.5 mmol of DIAD in 2.0 ml of anhydrous THF. The reaction was stirred overnight at room temperature after stirred at 0 °C for 1 hour. After distilled off the volatile solvents, the residue was dissolved by ethyl acetate and washed with brine for about 5 times and dried over anhydrous Na_2SO_4 . Filtered organic solution was evaporated to dryness and the residue was purified by silica gel column chromatography (petroleum ether/ethyl acetate 1/1) to give **6** (61%) as a white solid; m.p. 140-142 °C. ^1H NMR (400 MHz, C_6D_6) δ 7.00 (dd, $J = 7.1, 1.8$ Hz, 1H), 5.93 (dd, $J = 5.6, 2.5$ Hz, 1H), 4.89-4.84 (m, 1H), 4.56 (dd, $J = 11.3, 6.2$ Hz, 1H), 4.41 (d, $J = 1.7$ Hz, 1H), 4.22 (dd, $J = 11.3, 1.9$ Hz, 1H), 3.94 (d, $J = 11.6$ Hz, 1H), 3.49 (dd, $J = 8.4, 3.9$ Hz, 1H), 3.16 (d, $J = 11.6$ Hz, 1H), 2.55-2.31 (m, 3H), 2.10 (s, 3H), 1.98 (dd, $J = 12.2, 6.4$ Hz, 2H), 1.91-1.83 (m, 1H), 1.83-1.64 (m, 3H), 1.39 (s, 3H), 1.35 (s, 3H), 1.28 (tdd, $J = 12.5, 8.2, 4.6$ Hz, 3H), 1.18 (s, 3H), 0.94 (s, 3H); ^{13}C NMR (101 MHz, C_6D_6) δ 168.7, 161.3, 152.0, 146.9, 142.5, 126.4, 123.9, 115.3, 108.3, 80.3, 77.3, 71.8, 70.3, 64.0, 55.7, 55.2, 42.8, 39.0, 37.7, 36.9, 28.1, 25.8, 23.7,

22.7, 15.1; ESI-HRMS: m/z 455.2397 $[M+Na]^+$, calcd for $C_{25}H_{36}NaO_6$, 455.2410.

Preparation of 14 β -acetoxy-andrographolide (7)

0.5 mmol of Compound **6** was dissolved in 4 ml of methanol and then treated with 0.05 mmol of TsOH at 20 °C for 30 min. Diluted by ethyl acetate and washed with sat $NaHCO_3$, brine, the organic phase was dried over anhydrous Na_2SO_4 , filtered, evaporated by rotavapor to dryness. Compound **7** was purified by silica gel column chromatography (petroleum ether/ethyl acetate 10/7) (white solid, 93%, m.p. 163-165 °C). 1H NMR (400 MHz, $CDCl_3$) δ 6.98 (dd, $J = 7.0, 1.8$ Hz, 1H), 5.91 (dt, $J = 6.0, 1.8$ Hz, 1H), 4.85 (q, $J = 1.3$ Hz, 1H), 4.54 (dd, $J = 11.3, 6.1$ Hz, 1H), 4.36 (d, $J = 1.7$ Hz, 1H), 4.20 (ddd, $J = 25.9, 11.0, 1.8$ Hz, 2H), 3.46 (dt, $J = 10.2, 4.6$ Hz, 1H), 3.36–3.26 (m, 1H), 3.00–2.89 (m, 2H), 2.53–2.26 (m, 3H), 2.11 (s, 3H), 1.96 (td, $J = 12.5, 5.0$ Hz, 1H), 1.89–1.75 (m, 4H), 1.75–1.68 (m, 1H), 1.36–1.12 (m, 6H), 0.66 (s, 3H); ^{13}C NMR (101 MHz, $CDCl_3$) δ 170.5, 169.1, 150.6, 146.8, 123.9, 108.4, 80.4, 71.7, 68.1, 64.1, 55.7, 55.2, 42.9, 39.0, 37.7, 36.9, 28.2, 28.2, 25.6, 23.7, 22.7, 20.8, 15.2; ESI-HRMS: m/z 415.2067 $[M+Na]^+$, calcd for $C_{22}H_{32}NaO_6$, 415.2097.

Preparation of 14 β -andrographolide (8)

0.5 mmol of Compound **6** was dissolved in 4 ml of methanol and then treated with 0.05 mmol of TsOH at 40-50 °C for 4 hours. Diluted by ethyl acetate and washed with sat $NaHCO_3$, brine, the organic phase was dried over anhydrous Na_2SO_4 , filtered, evaporated by rotavapor to dryness. Compound **8** was purified by silica gel column chromatography (dichloromethane/ethyl acetate 1/2) (white solid, 80%, m.p. 200-202 °C). 1H NMR (400 MHz, $DMSO-d_6$) δ 6.61 (ddd, $J = 7.9, 6.1, 1.8$ Hz, 1H), 5.64 (d, $J = 6.1$ Hz, 1H), 5.06 (d, $J = 4.8$ Hz, 1H), 4.94 (t, $J = 6.1$ Hz, 1H), 4.79 (d, $J = 1.8$ Hz, 1H), 4.45–4.36 (m, 2H), 4.12 (dd, $J = 7.6, 2.8$ Hz, 1H), 4.02 (dd, $J = 9.9, 2.2$ Hz, 1H), 3.84 (dd, $J = 10.9, 2.9$ Hz, 1H), 3.24 (ddd, $J = 14.8, 9.9, 6.1$ Hz, 2H), 2.63–2.53 (m, 1H), 2.43–2.26 (m, 2H), 1.92 (t, $J = 12.2$ Hz, 2H), 1.79–1.59 (m, 4H), 1.43–1.15 (m, 3H), 1.08 (s, 3H), 0.66 (s, 3H); ^{13}C NMR (101 MHz, C_6D_6) δ 175.2, 153.3, 151.8, 134.5, 113.0, 83.8, 79.6, 70.2, 68.0, 60.7, 59.8, 47.6, 44.1, 42.9, 41.8, 33.2, 29.8, 29.3, 28.4, 20.2; ESI-HRMS: m/z 373.1981 $[M+Na]^+$, calcd for $C_{20}H_{30}NaO_5$, 373.1991.

Preparation of 3,19-acetonylidene-14 β -andrographolide (9)

The same procedure was used as the preparation of compound **5**. The compound **9** was purified by silica gel column with petroleum ether/ethyl acetate 10/7 as a white solid (90%), m.p. 167-168 °C. 1H NMR (400 MHz, $CDCl_3$) δ 6.95 (ddd, $J = 8.0, 6.5, 1.8$ Hz, 1H), 5.08 (t, $J = 6.5$ Hz, 1H), 4.87 (t, $J = 1.5$ Hz, 1H), 4.47 (dd, $J = 10.5, 6.1$ Hz, 1H), 4.43 (q, $J = 1.3$ Hz, 1H), 4.25 (dd, $J = 10.5, 2.1$ Hz, 1H), 3.96 (d, $J = 11.6$ Hz, 1H), 3.50 (dd, $J = 8.6, 3.6$ Hz, 1H), 3.18 (d, $J = 11.6$ Hz, 1H), 2.72–2.61 (m, 1H), 2.54–2.44 (m, 1H), 2.41 (dt, $J = 13.3, 2.9$ Hz, 1H), 2.07 (d, $J = 6.8$ Hz, 1H), 2.05–1.89 (m, 3H), 1.85–1.70 (m, 3H), 1.41 (s, 3H), 1.37 (s, 3H), 1.36–1.24 (m, 3H), 1.21 (s, 3H), 0.96 (s, 3H); ^{13}C NMR (101 MHz, $DMSO$) δ 169.8, 147.8, 146.3, 129.2, 108.1, 98.2, 75.8, 74.2, 64.8, 62.8, 55.2, 51.5, 38.2, 37.2, 37.1, 33.8, 27.4, 25.8, 25.2, 24.8, 24.6, 22.7, 15.8; ESI-HRMS: m/z 413.2302, $[M+Na]^+$, calcd for $C_{23}H_{34}NaO_5$, 413.2304.

Preparation of the series compounds 10a-10i, 11b and 11g

The same procedure was used as the preparation of 3,19-acetonylidene 14 β -acetoxy andrographolide (**6**). Generally, the purification was conducted by silica gel column with petroleum ether/ethyl acetate from 3/1 to 1/1.

3,19-Acetonylidene-14 β -phenoxy-andrographolide (10a)

From **5** in 51% yield, white solid, m.p. 153-155 °C. 1H NMR (400 MHz, $CDCl_3$) δ (ppm) 7.39–7.28 (m, 2H), 7.13 (td, $J = 7.4, 1.8$ Hz, 1H), 7.05 (tt, $J = 7.5, 1.0$ Hz, 1H), 6.88–6.80 (m, 2H), 5.53 (d, $J = 5.7$ Hz, 1H), 4.87 (d, $J = 1.6$ Hz, 1H), 4.60 (dd, $J = 10.7, 5.8$ Hz, 1H), 4.46 (s, 1H), 4.40 (dd, $J = 10.7, 2.0$ Hz, 1H), 3.91 (d, $J = 11.6$ Hz, 1H), 3.42 (dd, $J = 8.3, 3.9$ Hz, 1H), 3.14 (d, $J = 11.5$ Hz, 1H), 2.57–2.46 (m, 1H), 2.45–2.26 (m, 2H), 1.95 (dd, $J = 27.6, 12.1$ Hz, 2H), 1.88–1.77 (m, 1H), 1.75–1.67 (m, 1H), 1.64 (dd, $J = 11.8, 6.0$ Hz, 1H), 1.51 (dd, $J = 8.0, 5.4$ Hz, 1H), 1.37 (s, 3H), 1.34 (s, 3H), 1.31–1.19 (m, 3H), 1.17 (s, 3H), 0.87 (s, 3H); ^{13}C NMR (101 MHz, C_6D_6) δ 168.8, 157.0, 149.6, 148.1, 130.1, 126.0, 122.2, 115.9, 108.0, 99.4, 75.4, 71.5, 70.5, 64.2, 55.8, 51.3, 38.5, 38.3, 37.8, 33.7, 26.7, 26.1, 25.7, 25.3, 24.8, 23.3, 16.6; ESI-HRMS: m/z 489.2658 $[M+Na]^+$, calcd for $C_{29}H_{38}NaO_5$, 489.2617.

3,19-Acetonylidene-14 β -(4'-nitro-phenoxy)-andrographolide (10b)

From **5** in 52% yield, white solid, m.p. 179-181 °C. 1H NMR (400 MHz, $CDCl_3$) δ 8.31–8.22 (m, 2H), 7.19 (ddd, $J = 8.0, 6.7, 1.7$ Hz, 1H), 6.97–6.88 (m, 2H), 5.69–5.62 (m, 1H), 4.89 (dd, $J = 1.8, 1.0$ Hz, 1H), 4.67 (dd, $J = 10.9, 5.8$ Hz, 1H), 4.45 (d, $J = 1.5$ Hz, 1H), 4.37 (dd, $J = 10.9, 1.9$ Hz, 1H), 3.88 (d, $J = 11.6$ Hz, 1H), 3.44 (dd, $J = 7.8, 3.8$ Hz, 1H), 3.14 (d, $J = 11.5$ Hz, 1H), 2.54 (ddd, $J = 15.9, 7.8, 2.5$ Hz, 1H), 2.47–2.31 (m, 2H), 2.04–1.89 (m, 2H), 1.85–1.75 (m, 1H), 1.75–1.68 (m, 1H), 1.68–1.59 (m, 1H), 1.51 (td, $J = 8.0, 4.2$ Hz, 1H), 1.35 (s, 3H), 1.33 (s, 3H), 1.31–1.21 (m, 3H), 1.16 (s, 3H), 0.89 (s, 3H); ^{13}C NMR (101 MHz, $CDCl_3$) δ 168.68, 161.28, 151.98, 147.27, 142.53, 126.35, 123.93, 115.16, 108.26, 99.37, 75.42, 71.78, 70.26, 64.05, 55.82, 51.66, 38.50, 38.10, 37.58, 33.85, 26.47, 26.01, 25.94, 25.10, 24.43, 23.17, 16.44; ESI-HRMS: m/z 534.2473 $[M+Na]^+$, calcd for $C_{29}H_{37}NNaO_7$, 534.2468.

3,19-Acetonylidene-14 β -(3'-nitro-phenoxy)-andrographolide (10c)

From **5** in 32% yield, white solid, m.p. 163-165 °C. 1H NMR (400 MHz, C_6D_6) δ 7.51 (d, $J = 7.1$ Hz, 1H), 7.31 (d, $J = 2.1$ Hz, 1H), 7.23–7.16 (m, 1H), 6.62 (t, $J = 8.2$ Hz, 1H), 6.52 (dd, $J = 8.3, 1.8$ Hz, 1H), 4.85 (s, 1H), 4.62 (d, $J = 5.1$ Hz, 1H), 4.43 (s, 1H), 3.77 (d, $J = 11.6$ Hz, 1H), 3.67–3.54 (m, 2H), 3.41 (dd, $J = 7.1, 3.5$ Hz, 1H), 3.06 (d, $J = 11.5$ Hz, 1H), 2.12 (ddd, $J = 22.8, 17.7, 9.7$ Hz, 3H), 1.68 (dt, $J = 13.0, 6.6$ Hz, 2H), 1.53–1.36 (m, 2H), 1.39 (s, 3H), 1.35–1.25 (m, 2H), 1.34 (s, 3H), 1.07 (s, 3H), 0.99 (td, $J = 13.0, 3.8$ Hz, 1H), 0.94–0.80 (m, 2H), 0.84 (s, 3H); ^{13}C NMR (101 MHz, C_6D_6) δ 168.1, 157.1, 150.2, 149.5, 147.8, 130.4, 124.9, 122.2, 116.8, 109.2, 108.0, 99.5, 74.9, 71.8, 69.8, 64.2, 55.6, 51.0, 38.4, 38.2, 37.6, 33.5, 26.2, 25.9, 25.8, 25.1, 24.4, 23.1, 16.6; ESI-HRMS: m/z 534.2463 $[M+Na]^+$, calcd for $C_{29}H_{37}NNaO_7$, 534.2468.

3,19-Acetonylidene-14 β -(2'-nitro-phenoxy)-andrographolide (10d)

From **5** in 73% yield, white solid, m.p. 146-148 °C. 1H NMR (400 MHz, C_6D_6) δ 7.27 (dd, $J = 8.0, 1.7$ Hz, 1H), 7.21 (ddd, $J = 8.1,$

6.3, 1.9 Hz, 1H), 6.77–6.65 (m, 1H), 6.34 (td, $J = 7.8, 1.1$ Hz, 1H), 6.06–5.92 (m, 1H), 4.93–4.80 (m, 2H), 4.38 (t, $J = 2.8$ Hz, 1H), 3.82 (d, $J = 11.5$ Hz, 1H), 3.60 (qd, $J = 10.8, 4.2$ Hz, 2H), 3.45 (dd, $J = 7.7, 3.3$ Hz, 1H), 3.08 (d, $J = 11.5$ Hz, 1H), 2.40–2.29 (m, 1H), 2.26–2.11 (m, 2H), 1.86–1.67 (m, 2H), 1.62–1.47 (m, 3H), 1.42 (s, 3H), 1.36 (s, 3H), 1.36–1.31 (m, 1H), 1.12 (s, 3H), 1.05–0.91 (m, 3H), 0.87 (s, 3H); ^{13}C NMR (101 MHz, C_6D_6) δ 168.0, 151.6, 149.3, 148.4, 141.6, 133.2, 127.7, 125.8, 124.3, 121.7, 115.8, 107.8, 99.3, 75.4, 73.3, 69.6, 64.1, 55.7, 51.0, 38.4, 38.1, 37.6, 33.6, 26.7, 25.9, 25.2, 24.7, 23.2, 16.5; ESI-HRMS: m/z 534.2467 $[\text{M}+\text{Na}]^+$, calcd for $\text{C}_{29}\text{H}_{37}\text{NNaO}_7$, 534.2468.

Ethyl 3,19-acetonylidene-14 β -(2'-carboxy-phenoxy)-andrographolide (10e)

From **5** in 78% yield, white solid, m.p. 168–170 °C. ^1H NMR (400 MHz, C_6D_6) δ 7.80 (dd, $J = 7.7, 1.8$ Hz, 1H), 7.24–7.18 (m, 1H), 6.98–6.92 (m, 1H), 6.69 (td, $J = 7.6, 0.9$ Hz, 1H), 6.28 (d, $J = 8.2$ Hz, 1H), 5.04 (d, $J = 5.4$ Hz, 1H), 4.87–4.81 (m, 1H), 4.44 (s, 1H), 4.12 (qq, $J = 10.9, 7.1$ Hz, 2H), 4.01 (dd, $J = 10.6, 1.4$ Hz, 1H), 3.82 (d, $J = 11.5$ Hz, 1H), 3.68 (dd, $J = 10.6, 5.5$ Hz, 1H), 3.42 (dd, $J = 7.6, 3.7$ Hz, 1H), 3.08 (d, $J = 11.5$ Hz, 1H), 2.24–2.05 (m, 3H), 1.73 (dq, $J = 13.4, 6.8$ Hz, 2H), 1.59 (d, $J = 8.3$ Hz, 1H), 1.53–1.43 (m, 1H), 1.43–1.31 (m, 2H), 1.41 (s, 3H), 1.37 (s, 3H), 1.11 (s, 3H), 1.04 (t, $J = 7.1$ Hz, 3H), 1.01–0.89 (m, 3H), 0.85 (s, 3H); ^{13}C NMR (101 MHz, C_6D_6) δ 168.7, 165.7, 156.0, 149.7, 148.2, 132.9, 132.2, 127.8, 125.8, 123.9, 122.2, 116.6, 107.9, 99.3, 75.3, 73.2, 70.3, 64.1, 61.0, 55.8, 51.0, 38.4, 38.2, 37.6, 33.5, 26.6, 25.9¹, 25.8⁷, 25.2, 24.6, 23.2, 16.5, 14.1; ESI-HRMS: m/z 561.2829, $[\text{M}+\text{Na}]^+$, calcd for $\text{C}_{32}\text{H}_{42}\text{NaO}_7$, 561.2828.

3,19-Acetonylidene-14 β -(2'-methoxy-phenoxy)-andrographolide (10f)

From **5** in 60% yield, white solid, m.p. 130–131 °C. ^1H NMR (400 MHz, C_6D_6) δ 7.13–7.10 (m, 1H), 6.80 (td, $J = 7.8, 1.7$ Hz, 1H), 6.65 (td, $J = 7.7, 1.5$ Hz, 1H), 6.58 (dd, $J = 7.9, 1.6$ Hz, 1H), 6.47 (dd, $J = 8.1, 1.3$ Hz, 1H), 5.18 (d, $J = 5.4$ Hz, 1H), 4.82 (d, $J = 1.2$ Hz, 1H), 4.42 (s, 1H), 4.15 (dd, $J = 10.6, 1.5$ Hz, 1H), 3.83 (d, $J = 11.5$ Hz, 1H), 3.65 (dd, $J = 10.6, 5.5$ Hz, 1H), 3.41 (dd, $J = 7.7, 3.7$ Hz, 1H), 3.29 (s, 3H), 3.09 (d, $J = 11.5$ Hz, 1H), 2.26–2.04 (m, 3H), 1.83–1.62 (m, 2H), 1.54–1.28 (m, 10H), 1.08 (s, 3H), 1.05–0.82 (m, 6H); ^{13}C NMR (101 MHz, C_6D_6) δ 169.08, 151.78, 149.42, 148.27, 145.92, 128.15, 128.03, 127.91, 127.79, 127.67, 126.39, 124.00, 121.11, 120.16, 112.54, 107.85, 99.30, 75.39, 73.44, 70.56, 64.14, 55.72, 55.11, 51.10, 38.34, 38.12, 37.66, 33.56, 26.57, 26.00, 25.64, 25.29, 24.74, 23.24, 16.46; ESI-HRMS: m/z 519.2715 $[\text{M}+\text{Na}]^+$, calcd for $\text{C}_{30}\text{H}_{40}\text{NaO}_6$, 519.2723.

3,19-Acetonylidene-14 β -(2'-methoxy-4'-nitro-phenoxy)-andrographolide (10g)

From **5** in 51% yield, pale yellowish solid, m.p. 129–131 °C. ^1H NMR (400 MHz, C_6D_6) δ 7.56 (dd, $J = 8.8, 2.6$ Hz, 1H), 7.46 (d, $J = 2.6$ Hz, 1H), 7.20–7.15 (m, 1H), 5.95 (d, $J = 8.8$ Hz, 1H), 4.88 (d, $J = 5.5$ Hz, 1H), 4.83 (d, $J = 1.5$ Hz, 1H), 4.41–4.37 (m, 1H), 3.82–3.74 (m, 2H), 3.60 (dd, $J = 10.8, 5.7$ Hz, 1H), 3.41 (dd, $J = 7.3, 3.6$ Hz, 1H), 3.08 (s, 1H), 3.05 (s, 3H), 2.19–2.10 (m, 3H), 1.77–1.60 (m, 2H), 1.52–1.44 (m, 1H), 1.44–1.36 (m, 1H), 1.40 (s, 3H), 1.36 (s, 3H), 1.34–1.25 (m, 2H), 1.06 (s, 3H), 1.03–0.93 (m, 1H), 0.94–0.80 (m, 3H), 0.85 (s, 3H); ^{13}C NMR (101 MHz,

C_6D_6) δ 168.1, 150.8, 150.5, 150.3, 148.1, 143.2, 124.9, 116.9, 115.0, 107.7, 107.1, 99.4, 74.8, 72.9, 69.7, 64.0, 55.4, 55.1, 50.7, 38.2, 38.1, 37.4, 33.2, 26.1, 25.8, 25.6, 25.0, 24.3, 23.0, 16.4; ESI-HRMS: m/z 564.2584 $[\text{M}+\text{Na}]^+$, calcd for $\text{C}_{30}\text{H}_{39}\text{NNaO}_8$, 564.2573.

3,19-Acetonylidene-14 β -(2'-methyl-4'-nitro-phenoxy)-andrographolide (10h)

From **5** in 61% yield, white solid, m.p. 168–170 °C. ^1H NMR (400 MHz, C_6D_6) δ 8.13 (d, $J = 7.7$ Hz, 2H), 7.19 (td, $J = 7.2, 1.7$ Hz, 1H), 6.79–6.70 (m, 1H), 5.67 (d, $J = 5.6$ Hz, 1H), 4.91–4.84 (m, 1H), 4.67 (dd, $J = 10.9, 5.7$ Hz, 1H), 4.43 (d, $J = 1.8$ Hz, 1H), 4.35 (dd, $J = 11.0, 1.7$ Hz, 1H), 3.87 (d, $J = 11.6$ Hz, 1H), 3.43 (dd, $J = 7.7, 3.7$ Hz, 1H), 3.13 (d, $J = 11.6$ Hz, 1H), 2.51 (ddd, $J = 16.2, 7.4, 2.6$ Hz, 1H), 2.45–2.34 (m, 2H), 2.27 (s, 3H), 1.96 (ddd, $J = 27.0, 12.4, 6.9$ Hz, 2H), 1.83–1.66 (m, 2H), 1.65–1.44 (m, 3H), 1.34 (s, 3H), 1.33 (s, 3H), 1.31–1.17 (m, 3H), 1.15 (s, 3H), 0.89 (s, 3H); ^{13}C NMR (101 MHz, C_6D_6) δ 162.6, 153.7, 145.2, 142.7, 136.9, 123.1, 121.4, 119.4, 117.9, 105.4, 102.5, 94.2, 69.1, 66.5, 64.3, 58.8, 50.5, 45.4, 32.9, 32.2, 27.9, 20.5, 19.6, 18.7, 17.7, 11.4, 10.5; ESI-HRMS: m/z 548.2636, $[\text{M}+\text{Na}]^+$, calcd for $\text{C}_{30}\text{H}_{39}\text{NNaO}_7$, 548.2624.

3,19-Acetonylidene-14 β -(2'-fluoro-4'-nitro-phenoxy)-andrographolide (10i)

From **5** in 72% yield, white solid, m.p. 114–117 °C. ^1H NMR (400 MHz, C_6D_6) δ 7.56 (dd, $J = 10.6, 2.6$ Hz, 1H), 7.47 (ddd, $J = 9.1, 2.7, 1.5$ Hz, 1H), 7.23–7.18 (m, 1H), 5.75 (td, $J = 8.4, 3.3$ Hz, 1H), 4.84 (d, $J = 1.8$ Hz, 1H), 4.70 (d, $J = 5.1$ Hz, 1H), 4.39 (d, $J = 1.7$ Hz, 1H), 3.77 (d, $J = 11.6$ Hz, 1H), 3.63–3.51 (m, 2H), 3.43 (dd, $J = 7.0, 3.5$ Hz, 1H), 3.05 (d, $J = 11.5$ Hz, 1H), 2.26–2.08 (m, 3H), 1.79–1.60 (m, 2H), 1.55–1.43 (m, 2H), 1.39 (s, 3H), 1.34 (s, 3H), 1.36–1.27 (m, 2H), 1.05 (s, 3H), 1.01–0.85 (m, 3H), 0.89 (s, 3H); ^{13}C NMR (101 MHz, C_6D_6) δ 167.9, 167.7, 153.1, 151.5, 151.4, 150.6, 149.7, 149.6, 148.17, 142.3, 142.3, 124.2, 120.6, 115.0, 113.0, 112.8, 107.8, 99.5, 74.7, 73.4, 69.5, 64.2, 55.5, 50.7, 38.3, 38.3, 37.5, 33.2, 26.0, 25.8(2C), 25.0, 24.2, 23.1, 16.7; ESI-HRMS: m/z 552.2418 $[\text{M}+\text{Na}]^+$, calcd for $\text{C}_{29}\text{H}_{36}\text{FNNaO}_7$, 552.2374.

3,19-Acetonylidene-14 α -(4'-nitro-phenoxy)-andrographolide (11b)

From **9** in 56% yield, white solid, m.p. 149–152 °C. ^1H NMR (400 MHz, Benzene- d_6) δ 7.80–7.74 (m, 2H), 6.39 (dd, $J = 9.5, 2.4$ Hz, 2H), 6.11 (dt, $J = 4.7, 1.9$ Hz, 1H), 5.49 (s, 1H), 5.20 (dt, $J = 10.7, 1.8$ Hz, 1H), 5.17–5.13 (m, 1H), 3.86 (d, $J = 11.5$ Hz, 1H), 3.68 (dd, $J = 3.3, 2.0$ Hz, 2H), 3.50 (dd, $J = 7.1, 3.4$ Hz, 1H), 3.09 (d, $J = 11.5$ Hz, 1H), 2.36–2.20 (m, 2H), 2.09–2.03 (m, 1H), 2.02–1.92 (m, 1H), 1.85 (dd, $J = 14.6, 10.6$ Hz, 1H), 1.81–1.63 (m, 3H), 1.51 (dd, $J = 12.6, 6.7$ Hz, 1H), 1.43 (s, 3H), 1.41 (s, 3H), 1.33 (ddt, $J = 6.9, 5.1, 2.9$ Hz, 1H), 1.12–0.97 (m, 2H), 1.03 (s, 3H), 1.02 (s, 3H); ^{13}C NMR (101 MHz, C_6D_6) δ 171.5, 162.4, 147.2, 145.7, 142.2, 134.0, 125.9, 115.0, 109.1, 99.5, 75.0, 73.0, 69.9, 64.3, 52.3, 51.4, 38.4, 38.3, 38.2, 33.9, 30.9, 26.2, 25.8, 25.2, 24.6, 23.4, 17.0; ESI-HRMS: m/z 534.2500, $[\text{M}+\text{Na}]^+$ calcd for $\text{C}_{29}\text{H}_{37}\text{NNaO}_7$, 534.2468.

3,19-Acetonylidene-14 α -(2'-methoxy-4'-nitro-phenoxy)-andrographolide (11g)

From **9** in 50% yield, white solid, m.p. 121–123 °C. ^1H NMR (400 MHz, C_6D_6) δ 7.56 (dd, $J = 8.8, 2.4$ Hz, 1H), 7.45 (d, $J = 2.5$ Hz,

1H), 7.14–7.10 (m, 1H), 6.07–5.99 (m, 1H), 4.90 (s, 1H), 4.82 (s, 1H), 4.61 (s, 1H), 3.81 (dd, $J = 13.3, 6.7$ Hz, 2H), 3.71 (dd, $J = 10.8, 5.9$ Hz, 1H), 3.46 (dd, $J = 7.5, 3.7$ Hz, 1H), 3.07 (t, $J = 6.6$ Hz, 4H), 2.41–2.24 (m, 1H), 2.22–2.05 (m, 2H), 1.85 (td, $J = 13.6, 6.4$ Hz, 1H), 1.79–1.67 (m, 1H), 1.62–1.52 (m, 1H), 1.52–1.28 (m, 9H), 1.06 (d, $J = 16.4$ Hz, 3H), 1.04–0.89 (m, 3H), 0.84–0.74 (m, 3H); ^{13}C NMR (101 MHz, C_6D_6) δ 168.17, 151.11, 150.60, 147.17, 143.51, 124.80, 116.98, 115.61, 109.33, 107.40, 99.44, 75.17, 73.37, 69.90, 64.12, 55.82, 55.21, 51.25, 38.16, 38.04, 37.64, 34.06, 26.32, 26.01, 25.32, 25.20, 24.69, 23.16, 16.39; ESI-HRMS: m/z 564.2569 $[\text{M}+\text{Na}]^+$, calcd for $\text{C}_{30}\text{H}_{39}\text{NNaO}_8$, 564.2573.

Preparation of the series compounds 12a–12i, 13b and 13g.

The same procedure was used as the preparation of compound 7. Generally, the purification was conducted by silica gel column with petroleum ether/ethyl acetate from 2/1 to 1/1.

14 β -Phenoxy-andrographolide (12a)

From **10a** in 86% yield, white solid, m.p. 164–166 °C. ^1H NMR (400 MHz, CDCl_3) δ 7.40–7.29 (m, 2H), 7.14–7.01 (m, 2H), 6.89–6.79 (m, 2H), 5.55–5.48 (m, 1H), 4.85 (dd, $J = 1.9, 1.0$ Hz, 1H), 4.60 (dd, $J = 10.7, 5.9$ Hz, 1H), 4.44–4.36 (m, 2H), 4.17–4.08 (m, 1H), 3.40 (dd, $J = 11.5, 4.3$ Hz, 1H), 3.29 (d, $J = 10.9$ Hz, 1H), 2.54–2.44 (m, 1H), 2.44–2.36 (m, 1H), 2.33–2.23 (m, 1H), 2.16 (d, $J = 26.3$ Hz, 3H), 1.97 (td, $J = 12.7, 10.7, 6.2$ Hz, 1H), 1.92–1.85 (m, 1H), 1.85–1.70 (m, 2H), 1.70–1.55 (m, 2H), 1.33–1.16 (m, 5H), 1.11 (td, $J = 13.5, 3.7$ Hz, 1H), 0.58 (s, 3H); ^{13}C NMR (101 MHz, C_6D_6) δ 169.5, 156.4, 150.8, 147.1, 130.0, 125.0, 122.3, 115.7, 108.2, 80.4, 71.3, 71.0, 64.1, 55.9, 55.1, 42.8, 39.0, 37.7, 36.8, 28.1, 25.6, 23.7, 22.7, 15.1; HRMS (ESI): m/z 449.2342 $[\text{M}+\text{Na}]^+$, calcd for $\text{C}_{26}\text{H}_{34}\text{NaO}_5$, 449.2304.

14 β -(4'-Nitro-phenoxy)-andrographolide (12b)

From **10b** in 89% yield, white solid, m.p. 184–186 °C. ^1H NMR (400 MHz, CDCl_3) δ 8.32–8.23 (m, 2H), 7.18–7.11 (m, 1H), 6.93 (d, $J = 9.2$ Hz, 2H), 5.63 (d, $J = 5.7$ Hz, 1H), 4.87 (s, 1H), 4.67 (dd, $J = 10.9, 5.8$ Hz, 1H), 4.43–4.32 (m, 2H), 4.13 (d, $J = 11.2$ Hz, 1H), 3.42 (dd, $J = 11.6, 4.3$ Hz, 1H), 3.29 (d, $J = 11.0$ Hz, 1H), 2.50 (dd, $J = 7.0, 2.7$ Hz, 1H), 2.46–2.37 (m, 1H), 2.32 (dd, $J = 10.7, 7.1$ Hz, 1H), 2.05 (s, 3H), 1.97 (dd, $J = 12.7, 5.2$ Hz, 1H), 1.90 (d, $J = 10.5$ Hz, 1H), 1.87–1.70 (m, 2H), 1.70–1.63 (m, 1H), 1.60 (dd, $J = 13.0, 3.5$ Hz, 1H), 1.34–1.18 (m, 5H), 1.13 (td, $J = 13.2, 3.8$ Hz, 1H), 0.60 (s, 3H); ^{13}C NMR (101 MHz, CDCl_3) δ 168.7, 161.3, 152.0, 146.9, 142.5, 126.4, 123.9, 115.3, 108.3, 80.3, 77.3, 71.8, 70.3, 64.0, 55.7, 55.2, 42.8, 39.0, 37.7, 36.9, 28.1, 25.8, 23.7, 22.7, 15.1; HRMS (ESI): m/z 494.2148, $[\text{M}+\text{Na}]^+$, calcd for $\text{C}_{26}\text{H}_{33}\text{NNaO}_7$, 494.2155.

14 β -(3'-nitro-phenoxy)-andrographolide (12c)

From **10c** in 92% yield, white solid, m.p. 144–146 °C. ^1H NMR (400 MHz, CDCl_3) δ 7.94 (ddd, $J = 8.2, 2.0, 0.9$ Hz, 1H), 7.69 (t, $J = 2.3$ Hz, 1H), 7.54 (t, $J = 8.2$ Hz, 1H), 7.20 (ddd, $J = 8.3, 2.6, 0.9$ Hz, 1H), 7.14 (td, $J = 7.1, 1.7$ Hz, 1H), 5.62 (dt, $J = 5.6, 1.7$ Hz, 1H), 4.87 (q, $J = 1.3$ Hz, 1H), 4.67 (dd, $J = 10.9, 5.7$ Hz, 1H), 4.45–4.35 (m, 2H), 4.12 (d, $J = 11.2$ Hz, 1H), 3.41 (ddd, $J = 11.7, 4.5, 1.3$ Hz, 1H), 3.29 (dd, $J = 11.2, 1.3$ Hz, 1H), 2.51 (ddd, $J = 16.1, 7.2, 3.0$ Hz, 1H), 2.46–2.38 (m, 1H), 2.37–2.23 (m, 4H), 1.98 (td, $J = 12.6, 4.9$ Hz, 1H), 1.93–1.87 (m, 1H), 1.87–1.79 (m, 1H), 1.79–1.69 (m, 1H), 1.62 (ddt, $J = 24.2, 13.1, 3.8$ Hz, 2H), 1.34–1.18 (m, 5H), 1.12 (td, $J = 13.2, 4.1$ Hz, 1H), 0.60 (s, 3H);

^{13}C NMR (101 MHz, CDCl_3) δ 168.9, 157.0, 151.7, 149.4, 146.9, 130.9, 124.2, 122.4, 117.3, 109.7, 108.3, 80.3, 71.9, 70.4, 64.1, 55.8, 55.2, 42.8, 39.00, 37.7, 36.9, 28.1, 25.7, 23.7, 22.7, 15.1; HRMS (ESI): m/z 494.2156 $[\text{M}+\text{Na}]^+$, calcd for $\text{C}_{26}\text{H}_{33}\text{NNaO}_7$, 494.2155.

14 β -(2'-nitro-phenoxy)-andrographolide (12d)

From **10d** in 86% yield, white solid, m.p. 167–168 °C. ^1H NMR (400 MHz, CDCl_3) δ 7.89 (dd, $J = 8.1, 1.6$ Hz, 1H), 7.62–7.55 (m, 1H), 7.18 (t, $J = 7.7$ Hz, 1H), 7.15–7.10 (m, 1H), 6.92 (d, $J = 8.3$ Hz, 1H), 5.64 (d, $J = 5.6$ Hz, 1H), 4.83 (s, 1H), 4.66 (dd, $J = 10.9, 6.0$ Hz, 1H), 4.44 (dd, $J = 10.9, 2.0$ Hz, 1H), 4.31 (s, 1H), 4.13 (d, $J = 11.2$ Hz, 1H), 3.43 (dd, $J = 11.5, 4.6$ Hz, 1H), 3.28 (d, $J = 11.1$ Hz, 1H), 2.56–2.45 (m, 1H), 2.38 (dd, $J = 13.2, 3.5$ Hz, 1H), 2.26 (ddd, $J = 16.5, 11.2, 7.8$ Hz, 1H), 2.09 (s, 3H), 1.98 (t, $J = 12.3$ Hz, 1H), 1.89 (d, $J = 10.4$ Hz, 1H), 1.85–1.78 (m, 1H), 1.78–1.63 (m, 2H), 1.59 (dt, $J = 13.0, 3.3$ Hz, 1H), 1.24 (s, 5H), 1.10 (td, $J = 13.2, 3.9$ Hz, 1H), 0.58 (s, 3H); ^{13}C NMR (101 MHz, CDCl_3) δ 168.7, 152.6, 149.4, 147.3, 141.1, 134.1, 126.3, 123.7, 122.3, 115.9, 108.1, 80.3, 73.1, 70.3, 64.1, 55.8, 54.9, 42.8, 38.9, 37.6, 36.5, 28.1, 25.8, 23.7, 22.6, 15.1; HRMS (ESI): m/z 494.2158, $[\text{M}+\text{Na}]^+$, calcd for $\text{C}_{26}\text{H}_{33}\text{NNaO}_7$, 494.2155.

Ethyl 14 β -(2'-carboxy-phenoxy)-andrographolide (12e)

From **10e** in 88% yield, white solid, m.p. 181–182 °C. ^1H NMR (400 MHz, CDCl_3) δ 7.88 (dd, $J = 7.8, 1.7$ Hz, 1H), 7.56–7.46 (m, 1H), 7.20–7.11 (m, 1H), 7.04 (ddd, $J = 7.7, 6.0, 1.6$ Hz, 1H), 6.91 (d, $J = 8.3$ Hz, 1H), 5.61 (d, $J = 5.3$ Hz, 1H), 4.83 (d, $J = 1.9$ Hz, 1H), 4.63–4.48 (m, 2H), 4.41–4.26 (m, 3H), 4.14 (d, $J = 11.1$ Hz, 1H), 3.41 (dt, $J = 11.7, 2.8$ Hz, 1H), 3.29 (d, $J = 10.9$ Hz, 1H), 2.47–2.25 (m, 4H), 2.17 (ddd, $J = 16.4, 11.2, 8.2$ Hz, 1H), 1.96 (td, $J = 12.6, 5.2$ Hz, 1H), 1.88–1.78 (m, 2H), 1.78–1.61 (m, 2H), 1.36 (t, $J = 7.1$ Hz, 3H), 1.32–1.16 (m, 5H), 1.04 (td, $J = 13.3, 3.9$ Hz, 1H), 0.56 (s, 3H); ^{13}C NMR (101 MHz, CDCl_3) δ 169.5, 165.7, 155.8, 150.9, 147.1, 133.4, 132.3, 124.9, 123.2, 122.6, 117.0, 108.2, 80.3, 73.4, 71.0, 64.1, 61.2, 55.8, 54.9, 42.8, 38.8, 37.6, 36.6, 28.1, 25.6, 23.7, 22.6, 15.1, 14.3; HRMS (ESI): m/z 521.2517, $[\text{M}+\text{Na}]^+$, calcd for $\text{C}_{29}\text{H}_{39}\text{NaO}_7$, 521.2515.

14 β -(2'-methoxy-phenoxy)-andrographolide (12f)

From **10f** in 93% yield, white solid, m.p. 176–178 °C. ^1H NMR (400 MHz, CDCl_3) δ 7.13–7.02 (m, 1H), 7.01–6.83 (m, 4H), 5.58 (t, $J = 13.3$ Hz, 1H), 4.82 (t, $J = 7.3$ Hz, 1H), 4.55–4.40 (m, 2H), 4.32 (dd, $J = 7.6, 6.7$ Hz, 1H), 4.13 (t, $J = 8.9$ Hz, 1H), 3.92–3.81 (m, 3H), 3.47–3.35 (m, 1H), 3.30 (d, $J = 11.1$ Hz, 1H), 2.42–2.33 (m, 1H), 2.32–2.21 (m, 2H), 2.02–1.66 (m, 5H), 1.56 (dt, $J = 13.3, 3.6$ Hz, 1H), 1.31–1.02 (m, 6H), 0.61 (dd, $J = 18.6, 2.5$ Hz, 3H); ^{13}C NMR (101 MHz, CDCl_3) δ 169.77, 151.35, 150.68, 147.23, 145.29, 125.46, 124.33, 121.09, 119.97, 112.35, 108.12, 80.45, 73.42, 71.20, 64.14, 55.80, 55.69, 55.03, 42.87, 38.88, 37.69, 36.64, 28.22, 25.55, 23.73, 22.70, 15.10; HRMS (ESI): m/z 479.2408 $[\text{M}+\text{Na}]^+$, calcd for $\text{C}_{27}\text{H}_{36}\text{NaO}_6$, 479.2410.

14 β -(2'-methoxy-4'-nitro-phenoxy)-andrographolide (12g)

From **10g** in 87% yield, pale yellowish solid, m.p. 151–153 °C. ^1H NMR (400 MHz, CDCl_3) δ 8.13 (d, $J = 7.1$ Hz, 2H), 7.16 (q, $J = 7.0, 6.5$ Hz, 1H), 6.75 (d, $J = 9.6$ Hz, 1H), 5.64 (d, $J = 5.4$ Hz, 1H), 4.86 (s, 1H), 4.67 (dd, $J = 10.9, 5.7$ Hz, 1H), 4.39–4.32 (m, 2H), 4.12 (d, $J = 11.1$ Hz, 1H), 3.39 (dd, $J = 11.7, 4.3$ Hz, 1H), 3.29 (d, $J = 11.2$ Hz, 1H), 2.54–2.38 (m, 2H), 2.31 (d, $J = 32.5$ Hz, 5H), 2.11 (s, 3H), 1.97 (dt, $J = 13.0, 6.4$ Hz, 1H), 1.92–1.77

(m, 2H), 1.78–1.68 (m, 1H), 1.68–1.60 (m, 1H), 1.57 (dd, $J = 12.9, 3.3$ Hz, 1H), 1.34–1.15 (m, 5H), 1.08 (td, $J = 13.4, 3.6$ Hz, 1H), 0.59 (s, 3H); ^{13}C NMR (101 MHz, CDCl_3) δ 169.0, 151.8, 151.0, 150.6, 147.1, 143.3, 124.4, 117.4, 116.0, 108.2, 107.5, 80.4, 73.3, 70.6, 64.0, 56.4, 55.7, 55.1, 42.8, 38.9, 37.6, 36.6, 28.2, 25.7, 23.7, 22.8, 15.1; HRMS (ESI): m/z 524.2254, $[\text{M}+\text{Na}]^+$, calcd for $\text{C}_{27}\text{H}_{35}\text{NNaO}_8$, 524.2260.

14 β -(2'-methyl-4'-nitro-phenoxy)-andrographolide (12h)

From **10h** in 87% yield, white solid, m.p. 115–117 °C. ^1H NMR (400 MHz, CDCl_3) δ 8.13 (d, $J = 7.7$ Hz, 2H), 7.19 (td, $J = 7.2, 1.7$ Hz, 1H), 6.79–6.70 (m, 1H), 5.67 (d, $J = 5.6$ Hz, 1H), 4.91–4.84 (m, 1H), 4.67 (dd, $J = 10.9, 5.7$ Hz, 1H), 4.43 (d, $J = 1.8$ Hz, 1H), 4.35 (dd, $J = 11.0, 1.7$ Hz, 1H), 3.87 (d, $J = 11.6$ Hz, 1H), 3.43 (dd, $J = 7.7, 3.7$ Hz, 1H), 3.13 (d, $J = 11.6$ Hz, 1H), 2.51 (ddd, $J = 16.2, 7.4, 2.6$ Hz, 1H), 2.45 – 2.34 (m, 2H), 2.27 (s, 3H), 1.96 (ddd, $J = 27.0, 12.4, 6.9$ Hz, 2H), 1.83 – 1.66 (m, 2H), 1.65–1.44 (m, 3H), 1.33 (d, $J = 6.2$ Hz, 6H), 1.31–1.17 (m, 3H), 1.15 (s, 3H), 0.89 (s, 3H); ^{13}C NMR (101 MHz, CDCl_3) δ 168.7, 152.6, 149.3, 147.2, 141.0, 134.1, 126.2, 123.6, 122.3, 115.8, 108.0, 80.3, 73.1, 70.3, 64.1, 55.7, 54.8, 42.7, 38.8, 37.6, 36.5, 28.1, 25.8, 23.6, 22.6, 15.1; HRMS (ESI): m/z 508.2305, $[\text{M}+\text{Na}]^+$, calcd for $\text{C}_{27}\text{H}_{35}\text{NNaO}_7$, 508.2311.

14 β -(2'-fluoro-4'-nitro-phenoxy)-andrographolide (12i)

From **10i** in 91% yield, white solid, m.p. 162–165 °C. ^1H NMR (400 MHz, CD_3OD) δ 8.20–8.12 (m, 2H), 7.35 (t, $J = 8.4$ Hz, 1H), 7.14–7.05 (m, 1H), 6.04–5.98 (m, 1H), 4.91(s, 1H), 4.73 (dd, $J = 11.2, 5.5$ Hz, 1H), 4.57 (s, 1H), 4.46 (dd, $J = 11.2, 1.4$ Hz, 1H), 4.03 (d, $J = 11.1$ Hz, 1H), 3.33 (d, $J = 1.2$ Hz, 1H), 3.22 (dd, $J = 11.8, 4.1$ Hz, 1H), 2.53 (ddd, $J = 15.3, 8.0, 3.2$ Hz, 1H), 2.46–2.35 (m, 2H), 2.08–1.93 (m, 2H), 1.84 (ddt, $J = 12.5, 4.6, 2.3$ Hz, 1H), 1.74–1.47 (m, 3H), 1.34 (qd, $J = 12.8, 4.1$ Hz, 1H), 1.23 (dd, $J = 12.9, 2.3$ Hz, 1H), 1.18 (s, 3H), 1.11–0.99 (m, 1H), 0.65 (s, 3H); ^{13}C NMR (101 MHz, CD_3OD) δ 171.0, 154.4, 153.0, 151.9, 151.8, 151.7, 148.9, 143.4, 143.3, 126.1, 122.2, 122.2, 116.7, 113.8, 113.6, 108.5, 80.8, 74.6, 72.2, 64.9, 57.7, 56.3, 43.6, 40.2, 38.9, 37.9, 28.9, 26.8, 25.2, 23.4, 15.4; HRMS (ESI): m/z 512.2099 $[\text{M}+\text{Na}]^+$, calcd for $\text{C}_{26}\text{H}_{32}\text{FNNaO}_7$, 512.2061.

14 α -(4'-nitro-phenoxy)-andrographolide (13b)

From **11b** in 82% yield, white solid, m.p. 163–166 °C. ^1H NMR (400 MHz, C_6D_6) δ 8.18 – 8.13 (m, 2H), 7.25 (m, 1H), 6.91–6.86 (m, 2H), 5.21 (d, $J = 10.4$ Hz, 1H), 5.00 (d, $J = 6.9$ Hz, 2H), 4.84–4.79 (m, 2H), 4.18 (d, $J = 11.1$ Hz, 1H), 3.54–3.46 (m, 1H), 3.32 (d, $J = 11.1$ Hz, 1H), 2.48 (s, 1H), 2.43–2.35 (m, 1H), 2.13–2.02 (m, 1H), 1.96–1.76 (m, 6H), 1.43–1.14 (m, 6H), 1.25 (s, 3H), 1.23 (s, 3H), 0.66 (s, 3H); ^{13}C NMR (101 MHz, C_6D_6) δ 171.54, 162.43, 147.22, 145.74, 142.21, 134.02, 125.95, 115.01, 109.07, 99.53, 74.96, 72.97, 69.92, 64.28, 52.29, 51.37, 38.36, 38.27, 38.16, 33.92, 30.89, 26.20, 25.85, 25.16, 24.63, 23.45, 16.98; HRMS (ESI): m/z 494.2185, $[\text{M}+\text{Na}]^+$, calcd for $\text{C}_{29}\text{H}_{37}\text{NNaO}_7$, 494.2155.

14 α -(2'-methoxy-4'-nitro-phenoxy)-andrographolide (13g)

From **13g** in 79% yield, white solid, m.p. 155–159 °C. ^1H NMR (400 MHz, CD_3OD) δ 7.93 (dd, $J = 8.8, 2.6$ Hz, 1H), 7.90 (d, $J = 2.6$ Hz, 1H), 7.14 (d, $J = 8.8$ Hz, 1H), 7.05 (dd, $J = 9.7, 3.6$ Hz, 1H), 5.85 (d, $J = 5.7$ Hz, 1H), 4.89 (s, 1H), 4.71 (dd, $J = 10.9, 5.8$ Hz, 1H), 4.65 (s, 1H), 4.44 (dd, $J = 10.9, 1.8$ Hz, 1H), 4.08 (d, $J =$

11.1 Hz, 1H), 3.96 (s, 3H), 3.36 (t, $J = 5.4$ Hz, 2H), 2.56–2.38 (m, 3H), 2.08–1.93 (m, 2H), 1.85 (dd, $J = 12.8, 2.5$ Hz, 1H), 1.78–1.58 (m, 3H), 1.36 (ddd, $J = 25.0, 12.5, 4.0$ Hz, 1H), 1.30–1.15 (m, 5H), 0.64 (s, 3H); ^{13}C NMR (101 MHz, CD_3OD) δ 171.45, 153.12, 152.55, 151.94, 148.73, 144.44, 126.18, 118.28, 116.58, 109.47, 108.45, 80.89, 74.76, 72.59, 64.92, 57.18, 56.87, 56.30, 43.66, 39.85, 38.88, 38.16, 28.97, 26.37, 25.18, 23.36, 15.44; HRMS (ESI): m/z :524.2253 $[\text{M}+\text{Na}]^+$, calcd for $\text{C}_{27}\text{H}_{35}\text{NNaO}_8$, 524.2260.

General information for assay

Every compound was dissolved in DMSO and diluted with PBS into a stock solution before use. The final concentration of DMSO is 0.1% for all wells. Every experiment is in triplicate. Cell culture: 293T cells were maintained in MEM media with 10% fetal bovine serum (FBS), 100 U/mL penicillin and streptomycin and 1 mM non-essential amino acid under humidified air containing 5% CO_2 at 37 °C.

Transient transfection and FXR luciferase reporter assay³¹

293T cells were plated in 96-well plates at 2.5×10^4 per well. After cells attached, 5.0 ng/well pCMV-GAL4-DBD-hFXR-LBD expression vector, 25.0 ng/well pFRLuciferase and 5.0 ng/well Renilla-Luciferase reporter plasmids were transiently transfected into cells using 0.25 μL /well lipofectamine (Invitrogen). After transfection for 18 h, cells were treated with an FXR natural agonist chenodeoxycholic acid (CDCA) at 25 μM in fresh MEM containing 0.5% charcoal-stripped FBS. Then, synthesized compound was added in gradient concentrations in an antagonist mode. Luciferase activity was measured after an additional 24 h using Dual-Luciferase Reporter Assay System (Promega). The relative antagonistic activity was defined as the ratio of pFRLuciferase activity/Renilla-Luciferase activity and the activity of FXR in the presence of 25.0 μM of CDCA was set as 100%.

Cell viability assay for CC₅₀

293T cells were plated in 96-well plates at 2.5×10^4 per well. After cultured overnight, the cells were exposed to fresh medium containing different concentrations of synthesized compound. After cultured for additional 24 h, cell viability was determined by 3-(4,5-dimethylthiazol-2-yl)-2,5-diphenyltetrazolium bromide (MTT) assay.

The molecular docking of compounds 10b, 12b, 10g and 12g

The Molecular docking was performed using the Lamarckian Genetic Algorithm as implemented in Autodock 4.2. The crystal structure of the target protein was retrieved from the Protein Data Bank (PDB entry: 3DCT⁴²). The docking grids (binding site) were prepared as 60*60*60 points with a grid pacing of 0.375 Å and centred on the original ligand of the crystal structure. The set of parameters was listed as following: the size of the population was 150 and the number of energy evaluations was set to 1.0×10^7 as the run terminates. For clustering the conformations, the root mean square deviation tolerance was 2.0. Two hundred independent docking runs were carried out for every ligand. ALL other parameters were set to default. Analysis of the results was performed using AutoDockTools and the docked structures were viewed using Discovery Studio 3.5 Client.

Acknowledgements

Authors thank Dr. Qian Li for his help of the molecular docking.

Notes and references

^a School of Pharmaceutical Sciences, Nanjing Tech University, Nanjing 211816, PR China. *Corresponding author. Tel: 86-25-58139415; E-mail: gczhou@njtech.edu.cn.

^b NeuMed Pharmaceuticals Limited, Shatin, N.T., Hong Kong, PR China. *Corresponding author. Tel: 852- 67487218, E-mail:

wongcw@neuemedpharma.com.hk.

^c College of Biotechnology and Pharmaceutical Engineering, Nanjing Tech University, Nanjing 211816, PR China.

[§] Current address: Department of Pharmaceutical and Chemical Engineering, Taizhou Polytechnic College, Taizhou 225300, Jiangsu, PR China

† Electronic Supplementary Information (ESI) available: Tabel s1, ¹H NMR and ¹³C NMR spectra of compounds 5–13. See DOI: 10.1039/b000000x/

‡ The crystal structure of **10b** was deposited at the Cambridge Crystallographic Data Centre and deposition numbers is CCDC 960845.

- B. M. Forman, E. Goode, J. Chen, A. E. Oro, D. J. Bradley, T. Perlmann, D. J. Noonan, L. T. Burka, T. McMorris, W. W. Lamph, E. M. Evans and C. Weinberger, *Cell*, 1995, **81**, 687.
- P. Lefebvre, B. Cariou, F. Lien, F. Kuipers and B. Staels, *Physiol. Rev.*, 2009, **89**, 147.
- H. Wang, J. Chen, K. Hollister, L. C. Sowers and B. M. Forman, *Mol. Cell*, 1999, **3**, 543.
- M. Makishima, A. Y. Okamoto, J. J. Repa, H. Tu, R. M. Learned, A. Luk, M. V. Hull, K. D. Lustig, D. J. Mangelsdorf and B. Shan, *Science*, 1999, **284**, 1362.
- D. J. Parks, S. G. Blanchard, R. K. Bledsoe, G. Chandra, T. G. Conslor, S. A. Kliewer, J. B. Stimmel, T. M. Willson, A. M. Zavacki, D. D. Moore and J. M. Lehmann, *Science*, 1999, **284**, 1365.
- R. Pellicciari, S. Fiorucci, E. Camaioni, C. Clerici, G. Costantino, P. R. Maloney, A. Morelli, D. J. Parks and T. M. Willson, *J. Med. Chem.*, 2002, **45**, 3569.
- S. M. Soisson, G. Parthasarathy, A. D. Adams, S. Sahoo, A. Sitlani, C. Sparrow, J. Cui and J. W. Becker, *Proc. Natl. Acad. Sci. U.S.A.*, 2008, **105**, 5337.
- P. R. Maloney, D. J. Parks, C. D. Haffner, A. M. Fivush, G. Chandra, K. D. Plunket, K. L. Creech, L. B. Moore, J. G. Wilson, M. C. Lewis, S. A. Jones and T. M. Willson, *J. Med. Chem.*, 2000, **43**, 2971.
- M. J. Evans, P. E. Mahaney, L. Borges-Marcucci, K. Lai, S. Wang, J. A. Krueger, S. Gardell, C. Huard, R. Martinez, G. P. Vlasuk and D. C. Harnish, *Am. J. Physiol. Gastrointest. Liver Physiol.*, 2009, **296**, G543.
- K. C. Nicolaou, R. M. Evans, A. J. Roecker, R. Hughes, M. Downes and J. A. Pfefferkorn, *Org. Biomol. Chem.*, 2003, **1**, 908.
- I. Dussault, R. Beard, M. Lin, K. Hollister, J. Chen, J.-H. Xiao, R. Chandraratna and B. M. Forman, *J. Biol. Chem.*, 2003, **278**, 7027.
- N. L. Urizar, A. B. Liverman, D. T. Dodds, F. V. Silva, P. Ordentlich, Y. Yan, F. J. Gonzalez, R. A. Heyman, D. J. Mangelsdorf and D. D. Moore, *Science*, 2002, **296**, 1703.
- A. K. Verma, P. Khemaria, J. Gupta, D. P. Singh, B. S. Joshi, R. Roy, A. K. Mishra and R. Pratap, *ARKIVOC*, 2010, **9**, 1.
- V. Sepe, G. Bifulco, B. Renga, C. D'Amore, S. Fiorucci and A. Zampella, *J. Med. Chem.*, 2011, **54**, 1314.
- J. Yu, J. L. Lo, L. Huang, A. Zhao, E. Metzger, A. Adams, P. T. Meinke, S. D. Wright and J. Cui, *J. Biol. Chem.*, 2002, **277**, 31441.
- S. J. Nam, H. Ko, M. Shin, J. Ham, J. Chin, Y. Kim, H. Kim, K. Shin, H. Choi and H. Kang, *Bioorg. Med. Chem. Lett.*, 2006, **16**, 5398.
- B. A. Carter, O. A. Taylor, D. R. Prendergast, T. L. Zimmerman, R. Von Furstenberg, D. D. Moore and S. J. Karpen, *Pediatr. Res.*, 2007, **62**, 301.
- R. Kaimal, X. Song, B. Yan, R. King and R. Deng, *J. Pharmacol. Exp. Ther.*, 2009, **330**, 125.
- M. Kainuma, M. Makishima, Y. Hashimoto and H. Miyachi, *Bioorg. Med. Chem.*, 2007, **15**, 2587.
- H. Huang, Y. Yu, Z. Gao, Y. Zhang, C. Li, X. Xu, H. Jin, W. Yan, R. Ma, J. Zhu, X. Shen, H. Jiang, L. Chen and J. Li, *J. Med. Chem.*, 2012, **55**, 7037.
- J. Y. Chiang, R. Kimmel, C. Weinberger and D. Stroup, *J. Biol. Chem.*, 2000, **275**, 10918.
- P. A. Edwards, H. R. Kast and A. M. Anisfeld, *J. Lipid Res.*, 2002, **43**, 2.
- N. Y. Kalaany and D. J. Mangelsdorf, *Annu. Rev. Physiol.*, 2006, **68**, 159.
- W. Huang, K. Ma, J. Zhang, M. Qatanani, J. Cuvillier, J. Liu, B. Dong, X. Huang and D. Moore, *Science*, 2006, **312**, 233.
- F. Yang, X. Huang, T. Yi, Y. Yen, D. D. Moore and W. Huang, *Cancer Res.*, 2007, **67**, 863.
- S. Fiorucci, A. Mencarelli, E. Distrutti, G. Palladino and S. Cipriani, *Curr. Med. Chem.*, 2010, **17**, 139.
- S. Fiorucci, S. Cipriani, F. Baldelli and A. Mencarelli, *Prog. Lipid Res.*, 2010, **49**, 171.
- S. Fiorucci, S. Cipriani, A. Mencarelli, F. Baldelli, G. Bifulco and A. Zampella, *Mini-Rev. Med. Chem.*, 2011, **11**, 753.
- T. A. M. Gulder and B. S. Moore, *Curr. Opin. Microbiol.*, 2009, **12**, 252.
- K.-H. Lee, *J. Nat. Prod.*, 2010, **73**, 500.
- W. Liu and C.-W. Wong, *Phytother. Res.*, 2010, **24**, 369.
- M. K. Gorter, *Recl. Trav. Chim.*, 1911, **30**, 151.
- M. P. Cava, W. R. Chan, L. J. Haynes, L. F. Johnson and B. Weinstein, *Tetrahedron*, 1962, 397.
- T. Zhang, *Zhong Yao Cai*, 2000, **23**, 366.
- X. Liu, Y. Wang and G. Li, *Zhong Yao Cai*, 2003, **26**, 135.
- G.-Z. Liu, H.-W. Xu, K. Sun, J. Wang and H.-M. Liu, *J. Org. Chem.*, 2008, **28**, 201 and references therein.
- B. Das, C. Chowdhury, D. Kumar, R. Sen, R. Roy, P. Das and M. Chatterjee, *Bioorg. Med. Chem. Lett.*, 2010, **20**, 6947.
- Z. Wang, P. Yu, G. Zhang, L. Xu, D. Wang, L. Wang, X. Zeng and Y. Wang, *Bioorg. Med. Chem.*, 2010, **18**, 4269.
- J. C. Lim, T. K. Chan, D. S. Ng, S. R. Sagineedu, J. Stanslas and W. S. Wong, *Clin Exp Pharmacol Physiol.*, 2012, **39**, 300 and references therein.
- B. Zhou, D. Zhang and X. Wu, *Mini Rev Med Chem.*, 2013, **13**, 298 and references therein.
- Some of compounds were published in the patent CN103224492 A 20130731 by Guo-Chun Zhou, Chi-Wai Wong, Zhuyun Liu, Dekuan Sheng, Xin Nie and Decai Wang.
- A. Akwabi-Ameyaw, J. Y. Bass, R. D. Caldwell, J. A. Caravella, L. Chen, K. L. Creech, D. N. Deaton, S. A. Jones, I. Kaldor, Y. Liu, K. P. Madauss, H. B. Marr, R. B. McFadyen, A. B. Miller, F. N. Iii, D. J. Parks, P. K. Spearing, D. Todd, S. P. Williams and G. B. Wisely, *Bioorg. Med. Chem. Lett.*, 2008, **18**, 4339.